

**NANO-PERLITE AS AN ALTERNATIVE REINFORCING FILLER TO SILICA
IN PDMS COMPOSITES**

By

Erim Ülkümen

Submitted to the Graduate School of Engineering and Natural Sciences

in partial fulfillment of

the requirements for the degree of

Master of Science

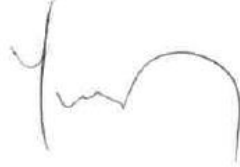
Sabancı University

May, 2013

NANO-PERLITE AS AN ALTERNATIVE REINFORCING FILLER TO SILICA IN
PDMS COMPOSITES

APPROVED BY

Prof. Dr. Yusuf Mencelođlu (Thesis Advisor)



Assist. Prof. Özge Akbulut



Assist. Prof. Fevzi Çakmak Cebeci



Assoc. Prof. Melih Papila



Prof. Dr. Ersin Serhatlı



DATE OF APPROVAL: 04/06/2013

© Erim Ülkümen 2013

All Rights Reserved

To my wife and grandfather...

NANO-PERLITE AS AN ALTERNATIVE REINFORCING FILLER TO SILICA IN PDMS COMPOSITES

Erim ÜLKÜMEN

MAT, Master of Science Thesis, 2013

Thesis Supervisor: Prof. Dr. Yusuf Menceoğlu

Keywords: Nano-perlite, Attrition mill, PDMS Composites

Abstract

Perlite is a highly potential national resource, and its use in silicone elastomer compounds as an alternative reinforcing filler to commercial grade fumed silica is targeted in this thesis work. Thus, comparative results are projected to be acquired. Expanded and raw perlite are characterized using X-Ray Diffraction (XRD), BET Surface Area Analyzer, Pycnometer and Scanning Electron Microscopy (SEM). Attrition mill is used to reduce particle size of expanded perlite. Dynamic Light Scattering (DLS) results showed that particle size was around 260 nm, whereas Scanning Electron Microscopy revealed particle size was between 40-50 nm. Using BET surface analysis and surface titration experiments, hydroxyl group density on expanded perlite surface was calculated, which came out to be 0.0406 -OH/nm^2 . Perlite and PDMS masterbatches were prepared using a high-speed mixer and mechanical and rheological properties of the elastomers cured from the masterbatches were studied using a Universal Testing Machine (UTM) and Rubber Process Analyzer (RPA 2000). Surface of the mineral was further modified using Hexamethyldisilazane, increasing wettability and mechanical properties of the elastomer samples. Rheological studies and SEM characterization showed a homogeneous distribution of the filler. As a result, surface modified nano expanded perlite exhibited uniform dispersity in the PDMS matrix, similar to commercial grade fumed silica, and their composites exhibited good mechanical properties.

NANO PERLİTİN SİLİKON KOMPOZİTLERDE SİLİKAYA ALTERNATİF OLARAK KULLANILMASI

Erim ÜLKÜMEN

MAT, Yüksek Lisans Tezi, 2013

Tez Danışmanı: Prof. Dr. Yusuf Menceoğlu

Anahtar Kelimeler: Nano-perlit, Attritör değirmen, PDMS Kompozit

Özet

Silikon karışımlarda güçlendirici dolgu malzemesi olarak kullanılmak üzere geliştirilmiş perlit kullanımı hedeflenmiştir. Endüstride yaygın olarak kullanılan silikaya alternatif olarak kullanılması planlanan perlitin getireceği avantajlar elde edilmiştir.

Attritör değirmeni kullanılarak geliştirilmiş parçacık boyutu nano seviyeye indirilmiştir. Parçacık boyutu Dinamik Işık Saçılımı sonuçlarına göre 260 nm, Taramalı Elektron Mikroskopi sonuçlarına göre 40 ile 50 nm arasında tespit edilmiştir. BET yüzey analizi ve titrasyon çalışmalarına göre, perlit yüzeyindeki hidroksil grup miktarı tayin edilmiş, bu değer $0,0406 \text{ -OH/nm}^2$ olarak hesaplanmıştır. Mineralin yüzeyi hexametil disilazane kullanılarak iyileştirilmiş, perlitin matriks tarafından daha kolay ıslanması sağlanmış ve topaklanmanın önüne geçilerek elastomer formülasyonların mekanik özelliklerinde artış sağlanmıştır. Reolojik ve SEM karakterizasyonu perlit dağılımının homojen olduğunu göstermiştir. Sonuç olarak, perlit PDMS matriksi içerisinde iyi bir dağılım göstererek hazırlanan kompozitlerin mekanik mukavemetlerinin arttığı gözlenmiştir.

ACKNOWLEDGMENTS

First of all, I would like thank to my supervisor Prof. Dr. Yusuf Mencelođlu for his guidance during my research and studies at Sabanci University. His guidance and motivations were invaluable for my research and thesis.

Secondly, I would like to thank our project partners for their support and guidance in this thesis work.

I would also like to thank the members of my advisory committee, Assoc. Prof. Melih Papila, Asst. Prof. Fevzi akmak Cebeci, Asst. Prof. zge Akbulut, and Prof. Ersin Serhatlı for reviewing my master thesis. I wish to extend my gratitude to all faculty members of Materials Science and Engineering Program.

I express special acknowledgement to Eren ŐimŐek, Kinyas Aydın, Aya Abakay, Mustafa Baysal, Kaan Bilge, Ođuzhan Ođuz, Ercan Gündođan, Hamidreza Khassaf, and Burcu Saner for their advices and wonderful friendship in Sabancı University. There are more people who have made Sabanci University a very special place: Firuze Okyay, zlem KocabaŐ, Ezgi Dündar Tekkaya, Sinem TaŐ, Göliz İnan, Elif zden, Gölcan orapođlu, zge Malay, Shalima Shawuti, Dilek akırođlu, Ashıhan rüm, Bahar Burcu Karahan, ađatay Yılmaz, Fazlı Fatih Melemez, Gökce Güven, Mariamu Kassim Ali, Cem Burak Kılı and Hale Nur ölođlu.

Finally, my deepest gratitude goes to my wife and family for their love and support.

Table of Contents

Abstract.....	1
Özet.....	2
Table of Contents.....	4
1. Introduction.....	11
2. Literature Review on Perlite and PDMS Composites.....	12
2.1. Perlite.....	12
2.2. PDMS Background.....	13
2.3. Silicone Elastomers in the Industry.....	15
3. Experimental.....	21
3.1. Perlite Preparation.....	21
3.1.1. Ball Milling.....	21
3.1.2. Screening.....	22
3.2. Perlite Characterization Experiments.....	22
3.2.1. Surface Titration.....	22
3.2.2. X-ray Diffraction Measurements (XRD).....	23
3.2.3. Pycnometer Measurements.....	23
3.2.4. BET Surface Test.....	23
3.2.5. SEM Analysis.....	23
3.3. Nano-Perlite Production Using Attrition Milling and Its Characterization.....	24
3.3.1. Dynamic Light Scattering Measurements (DLS).....	25
3.3.2. Scanning Electron Microscopy.....	25
3.4. Perlite Expansion Experiments.....	26
3.4.1. Expansion Using Laboratory Furnace.....	26
3.4.2. Hot Stage Microscopy.....	26
3.4.3. Pycnometer Analysis.....	26
3.5. Surface Modification of Nano-Perlite and its Characterization.....	26
3.5.1. Separating Nano-Perlite from Suspension.....	27
3.5.2. Grinding Nano-Perlite into Fine Powder.....	27
3.5.3. Fourier Transform Infrared Spectroscopy.....	27
3.5.4. Thermogravimetric Measurements.....	27
3.6. Masterbatch Preparation.....	28

3.7. Cured Elastomer Characterization.....	28
3.7.1. Universal Testing Machine Measurements.....	28
3.7.2. Rheology Measurements.....	29
4. Results/Discussions	30
4.1. Raw Perlite Preparation, Characterization, Expansion.....	30
4.1.1. Raw Perlite Preparation.....	30
4.1.2. Raw Perlite Characterization.....	31
4.1.2.1. XRD Analysis.....	31
4.1.2.2. BET Surface Analysis.....	32
4.1.2.3. Pycnometer Analysis.....	32
4.1.2.4. SEM Characterization.....	32
4.1.3. Raw Perlite Expansion and Characterization.....	33
4.1.3.1. Expansion Using Laboratory Furnace.....	33
4.1.3.2. SEM Analysis of Perlite Particles.....	33
4.2. Nano Raw Perlite Preparation, Characterization, Expansion.....	37
4.2.1. Nano Raw Perlite Preparation and Characterization.....	37
4.2.1.1. Attrition Mill Process.....	37
4.2.1.2. BET Surface Analysis.....	38
4.2.1.3. Optimization Study & Dynamic Light Scattering	40
4.2.1.4. SEM Characterization.....	40
4.2.2. Nano Raw Perlite Expansion and Characterization.....	42
4.2.2.1. Expansion Using Laboratory Furnace.....	42
4.2.2.2. SEM Analysis of Perlite Particles	42
4.2.2.3. Pycnometer and BET Surface Analysis.....	45
4.2.2.4. Expansion Using Hot Stage Microscopy.....	46
4.3. Expanded Perlite Preparation and Characterization.....	47
4.3.1. Expanded Perlite Preparation	47
4.3.2. Expanded Perlite Characterization.....	48
4.3.2.1. XRD Analysis.....	48
4.3.2.2. BET Surface Analysis.....	49
4.3.2.3. Pycnometer Analysis.....	49
4.3.2.4. SEM Characterization.....	49
4.3.2.5. Surface Titration.....	50

4.4. Nano Expanded Perlite Preparation and Characterization.....	51
4.4.1. Nano Expanded Perlite Preparation and Characterization.....	51
4.4.1.1. Attrition Mill Process.....	51
4.4.1.2. BET Surface Analysis.....	51
4.4.1.3. Pycnometer Analysis.....	51
4.4.1.4. Optimization Study & Dynamic Light Scattering.....	51
4.4.1.5. SEM Characterization.....	53
4.5. Surface Treated Nano Perlite Preparation and Characterization.	54
4.5.1. Surface Treated Nano Perlite Preparation.....	54
4.5.2. Surface Treated Nano Perlite Characterization.....	55
4.5.2.1. Fourier Transform Infrared Spectroscopy – FT-IR.....	55
4.5.2.2. Thermogravimetric Analysis.....	56
4.6. Masterbatch and Elastomer Preparation.....	57
4.6.1. Using Nano Raw Perlite.	57
4.6.1.1. Mixing PDMS and Perlite to Obtain Masterbatch.	57
4.6.1.2. Elastomer Formulation and Characterization.....	58
4.6.2. Using Expanded Perlite.....	61
4.6.2.1. Mixing PDMS and Perlite to Obtain Masterbatch.....	61
4.6.2.2. Elastomer Formulation and Characterization.....	61
4.6.3. Using Nano Expanded Perlite.....	64
4.6.3.1. Mixing PDMS and Perlite to Obtain Masterbatch.....	64
4.6.3.2. Elastomer Formulation and Characterization.....	64
4.6.4. Using Surface Modified Nano Expanded Perlite.....	67
4.6.4.1. Mixing PDMS and Perlite to Obtain Masterbatch.....	67
4.6.4.2. Elastomer Formulation and Characterization.....	68
4.7. Summary of Mechanical Results of Prepared Elastomers.....	75
5. Conclusion.....	78
5.1 Conclusion.....	78
5.2. Road Map.....	81

List of Figures

Figure 4.1: XRD Spectrum of Expanded Perlite (Particle size between 1-10 microns).....	31
Figure 4.2: BET system.....	32
Figure 4.3: Raw Perlite Particle at 4000 magnification	33
Figure 4.4: Raw Perlite (After 10 seconds).....	34
Figure 4.5: Raw Perlite (After 1 minute).....	34
Figure 4.6: Raw Perlite (After 2 minutes).....	35
Figure 4.7: Raw Perlite (After 10 minutes).....	35
Figure 4.8: Raw Perlite (After 10 minutes).....	36
Figure 4.9: Raw Perlite (After 30 minutes).....	36
Figure 4.10: Raw Perlite (After 30 minutes).....	37
Figure 4.11: DLS Spectrum of Raw Perlite after 60 minutes of Milling	39
Figure 4.12: DLS Spectrum of Raw Perlite after 90 minutes of Milling	39
Figure 4.13: DLS Spectrum of Expanded Perlite after 120 minutes of Milling.....	40
Figure 4.14: SEM Image of Ground Raw Perlite at 30000 Magnification	40
Figure 4.15: SEM Image of Ground Raw Perlite at 75000 Magnification	41
Figure 4.16: SEM Image of Ground Raw Perlite kept at 300°C for 10 minutes, 30000 Magnification.....	42
Figure 4.17: SEM Image of Ground Raw Perlite kept at 300°C for 10 minutes, 100000 Magnification	43
Figure 4.18: SEM Image of Ground Raw Perlite kept at 500°C for 10 minutes, 30000 Magnification.....	43
Figure 4.19: SEM Image of Ground Raw Perlite kept at 500°C for 10 minutes, 75000 Magnification.....	44
Figure 4.20: SEM Image of Ground Raw Perlite kept at 800°C for 10 minutes, 30000 Magnification.....	44
Figure 4.21: SEM Image of Ground Raw Perlite kept at 800°C for 10 minutes, 75000 Magnification	45
Figure 4.22: Expansion Character of Nano Raw Perlite (Taşper Ltd.)	47
Figure 4.23: Expansion Character of Raw Nano Perlite (Genper Ltd.).....	47
Figure 4.24: XRD Spectrum of Ground Perlite.....	49

Figure 4.25: Expanded Perlite Particle at 4000 Magnification.....	50
Figure 4.26: Expanded Perlite Particle at 10000 Magnification	50
Figure 4.27: DLS Spectrum of Expanded Perlite after 60 minutes of Milling.....	52
Figure 4.28: DLS Spectrum of Expanded Perlite after 90 minutes of Milling	52
Figure 4.29: DLS Spectrum of Expanded Perlite after 120 minutes of Milling.....	52
Figure 4.30: SEM Image of Ground Expanded Perlite at 20000 Magnification.....	53
Figure 4.31: SEM Image of Ground Expanded Perlite at 82000 Magnification.....	53
Figure 4.32: FT-IR Spectrum of Nano Expanded Perlite.....	55
Figure 4.33: FT-IR Spectrum of Nano Expanded Perlite after Hexamethyldisilazane Reaction and Being Dried at 100°C.....	55
Figure 4.34: TGA Analyses of Nano Expanded Perlite and Nano Expanded Perlite after Hexamethyldisilazane Reaction and Being Dried at 100°C.....	57
Figure 4.35: Target Masterbatch Frequency Sweep.....	59
Figure 4.36: Frequency Sweep of 10, 20 and 30 % Filled Masterbatches (Nano Raw Perlite + Methyl-terminated PDMS).....	60
Figure 4.38: Frequency Sweep of 10, 20 and 30 % Filled Masterbatches (Expanded Perlite + Methyl-terminated PDMS).....	63
Figure 4.40: Frequency Sweep of 10, 20 and 30 % Filled Masterbatches (Nano Expanded Perlite + Methyl-terminated PDMS).....	67
Figure 4.42: Frequency Sweep of 10, 20 and 30 % Filled Masterbatches (Surface Treated Nano Expanded Perlite + Methyl-terminated PDMS).....	70
Figure 4.43: SEM Image of Elastomer Formulation IV at 8000 Magnification Using Backscattered Electron Detector.....	71
Figure 4.44: SEM Image of Elastomer Formulation IV at 16000 Magnification Using Backscattered Electron Detector.....	72
Figure 4.45: SEM Image of Elastomer Formulation IV at 32000 Magnification Using Backscattered Electron Detector.....	72
Figure 4.46: SEM Image of Elastomer Formulation IV at 2000 Magnification Using Backscattered Electron Detector.....	73
Figure 4.47: SEM Image of Target Elastomer at 2000 Magnification Using Backscattered Electron Detector.....	74

Figure 4.48: SEM Image of Target Elastomer at 16000 Magnification Using Backscattered Electron Detector.....	74
Figure 4.49: Viscosity of Prepared Elastomers Using 4 Different Types of Perlite.....	75
Figure 4.50: Hardness of Prepared Elastomers Using 4 Different Types of Perlite.....	75
Figure 4.51: Tensile Strength of Prepared Elastomers Using 4 Different Types of Perlite.....	76
Figure 4.52: Elongation at Break of Prepared Elastomers Using 4 Different Types of Perlite.....	76
Figure 4.53: Tear Strength of Prepared Elastomers Using 4 Different Types of Perlite..	77

List of Tables

Table 2.1: Perlite Composition.....	12
Table 2.2: Brief Overview of Applications for Silicone Elastomers.....	16
Table 4.1: Attrition Mill optimization study recorded at constant feed rate and 1800 rpm.....	38
Table 4.2: Pycnometer Analysis of Heat Treated Nano Raw Perlite Samples.....	46
Table 4.3: Attrition Mill optimization study recorded at constant feed rate and 1800 rpm.....	52
Table 4.4: Mechanical Properties of Prepared Elastomers (Using Nano Raw Perlite)..	58
Table 4.5: Mechanical Properties of Prepared Elastomers (Using Expanded Perlite)..	62
Table 4.6: Mechanical Results of Prepared Elastomers (Using Nano Expanded Perlite).....	65
Table 4.7: Mechanical Results of Prepared Elastomers (Using Surface Modified Nano Expanded Perlite.....	68

CHAPTER 1

1. Introduction

Polydimethyl silicone (PDMS) comes from a group of thermally; physically and chemically stable polymers due to silicone-oxygen bonds in the backbone. PDMS has an extraordinary low glass transition temperature of around $-100\text{ }^{\circ}\text{C}$ mainly due to nature of silicon-oxygen bond. Silicone elastomers can be regularly produced when PDMS are cross-linked giving them low surface energy, temperature flexibility, clarity and physical and chemical stability. However, mechanical properties of silicone elastomers are very poor, resulting from the lack of intermolecular interactions due to low surface energy. Therefore, they must be reinforced to be used in the applications such as medical implants, sealants, automotive and cable. Fumed silica is a widely used reinforcing agent because of interactions between siloxane bonds in the backbone of PDMS and hydroxyl groups on silica surface. Although a lot of papers have been published investigating properties of these materials and the need of reinforcement, limited number of article mention compatibility and comparison of platelet perlite and spherical silica. We found that when reinforced PDMS with platelet fillers, the modulus of PDMS increase drastically due to high aspect ratio increasing mechanical properties such as tensile and tear strength; provide better matrix interaction and easier processability. In this thesis, the use of platelet perlite and spherical silica in silicone elastomer compounds as a filler loading material has been targeted. Platelet perlite is to be used as an alternative to amorphous silica, thus comparative results are projected to be acquired in terms of morphological, mechanical and rheological properties.

CHAPTER 2

2. Literature Review on Perlite and PDMS Composites

2.1. Perlite

Perlite is a glassy volcanic rock that contains 2–5 weight % water. When perlite is heated rapidly in the range 700–1,000°C it expands 10–15 times its original volume and leads to a lightly colored frothy material, expanded perlite. During the expansion process the grains start to soften superficially. At the pyroplastic stage, the water trapped into the inner layers of grains starts to evaporate and pushes its way out, resulting in the expansion of grains. Water plays the most important role in the expansion process not only by expanding the grain during evaporation but also by reducing the viscosity of the softened grain [1]. Expanded perlite exhibits increased porosity and decreased density. Representative values of density for crude, crashed and expanded perlite are 2.2–2.4, 0.9–1.1 and 0.6–1.2 kg/m³, respectively.

Table 2.1: Perlite Composition

SiO₂	Al₂O₃	CaO + MgO	Na₂O+K₂O
% 65.7–75.3	% 11-15	% 0.3-0.4	% 2-10

This versatile, lightweight material with its low bulk density continues to grow in popularity even though it is by no means the cheapest. Along the Aegean coast, Turkey possesses about 70% (70×10^9 tons) of the world's known perlite reserves. Over half of the perlite produced goes into the construction industry, in particular as aggregate in insulation board, plaster, and concrete. In industry, perlite is expanded in horizontal rotary or stationary furnaces or, mainly, in vertical expansion furnaces. Numerical simulations [2–4] as well as a theoretical analysis [5] of the expansion process have been reported for vertical furnaces. It was suggested that expansion occurs in less than 3 s after perlite is inserted into the high temperature furnace [2]. Although expansion is the most important treatment of perlite, research work on perlite is devoted mainly to properties [6–9] and potential uses [10–18] of this material. However, questions related to structural changes induced by thermal treatment, that may support a mechanism of expansion at a molecular level, remain open.

Water in perlite is present as molecular water and as hydroxyl groups [19]. Water in the form of hydroxyl groups bound to silicon atoms (i.e. in Si–OH bonds) is introduced into the silicate network under hydrothermal conditions [20]. The number of hydroxyl groups per silicon atom affects directly the connectivity of the perlite network, and this is usually expressed in terms of the Q^n silicate tetrahedral units with n being the number of oxygen atoms bridging two silicon centers. The concentration of hydroxyl groups in perlite increases with total water content. For total water content over 3 weight % the hydroxyl content may level off, while the concentration of molecular water increases [21].

2.2. PDMS Background

Recent developments in nanoscience and nanotechnology have spawned a wide range of novel and interesting materials, but the realization of practical utility has come relatively slowly in comparison. With that said, there are success stories, and polymer nanocomposites may be one of them, with numerous companies now producing such materials on an industrial scale. The interest in these materials stems from the ability of polymer nanocomposites (when thermodynamically compatible and effectively processed) to give rise to improvements in a wide range of materials properties (mechanical, thermal, barrier, fire, etc.) with the addition of only a small amount of nanofiller. A prerequisite is nanofiller dispersion; however, this statement alone is misleading, because it has been clearly shown that dispersion in the absence of thermodynamic compatibility does not give rise to property enhancements [22]. In compatible systems where dispersion is realized, on the other hand, there are several examples in the literature of systems whose overall ability to absorb mechanical energy, or toughness, has actually increased with the addition of layered silicate nanofillers, both in impact [23-25] and tension [26-29]. Such behavior, which is atypical of most filled polymers, indicates that, under the right circumstances (i.e., when homogeneity of dispersion and distribution are high and large agglomerates are rare or absent), dispersed nanoparticles are able to enhance the ability of the polymer matrix to dissipate energy. Such enhancements must originate from one of two factors: changes in polymer microstructure (alterations in crystalline phase, crystallite size and morphology, degree of crystallinity, confinement effects, cross-link/entanglement density, phase behavior in

multiphase systems, etc.) or interfacial stress transfer and modulations thereof (due to irreversible bond formation, reversible intermolecular interactions, interfacial slip, etc., with the importance of nanofiller size, shape, and properties implicit here). Beyond these concerns, there is also the matter of the matrix polymer chosen for this work, i.e., poly (dimethylsiloxane) (or PDMS). As a polysiloxane, or silicone, PDMS belongs to a family of unique polymers whose backbones consist entirely of silicon-oxygen bonds and are therefore highly physically, chemically, and thermally stable. The high ionic character of these bonds allows for very high levels of molecular flexibility, and, as a result, PDMS has an exceptionally low glass transition temperature of 146 K [30]. As liquids at room temperature, PDMS and several other linear silicones have found application as lubricants and heat-transfer fluids. Similarly, they are routinely cross-linked to produce silicone elastomers with excellent physical, chemical, and thermal stability; good low-temperature flexibility; clarity; and low surface energy. These find use in applications from sealants and caulking compound to nontoxic antifouling coatings for ships to microfluidics cells and medical implants for reconstructive surgery. However, the low surface energy of silicones such as PDMS implies a lack of intermolecular interactions, and this translates into one of the major weaknesses of silicone elastomers: their mechanical stability is so poor that they must be reinforced to be useful. Fumed silica, which consists of agglomerated aggregates of amorphous silica nanoparticles on the order of nanometers to tens of nanometers in size, has been one of the most favored reinforcing (nano) fillers for silicones, studied and used for decades, thanks to the strong hydrogen-bond mediated interactions between hydroxyl groups on the fumed silica surface and siloxane bonds in the PDMS backbone [31]. In contrast, while thousands of papers have been published on the subject of layered silicate nanocomposites, only a handful of detailed reports have focused on polysiloxanes, [32-41] despite the desirable properties of these materials, their need for reinforcement, and their compatibility with silica-based nanofillers.

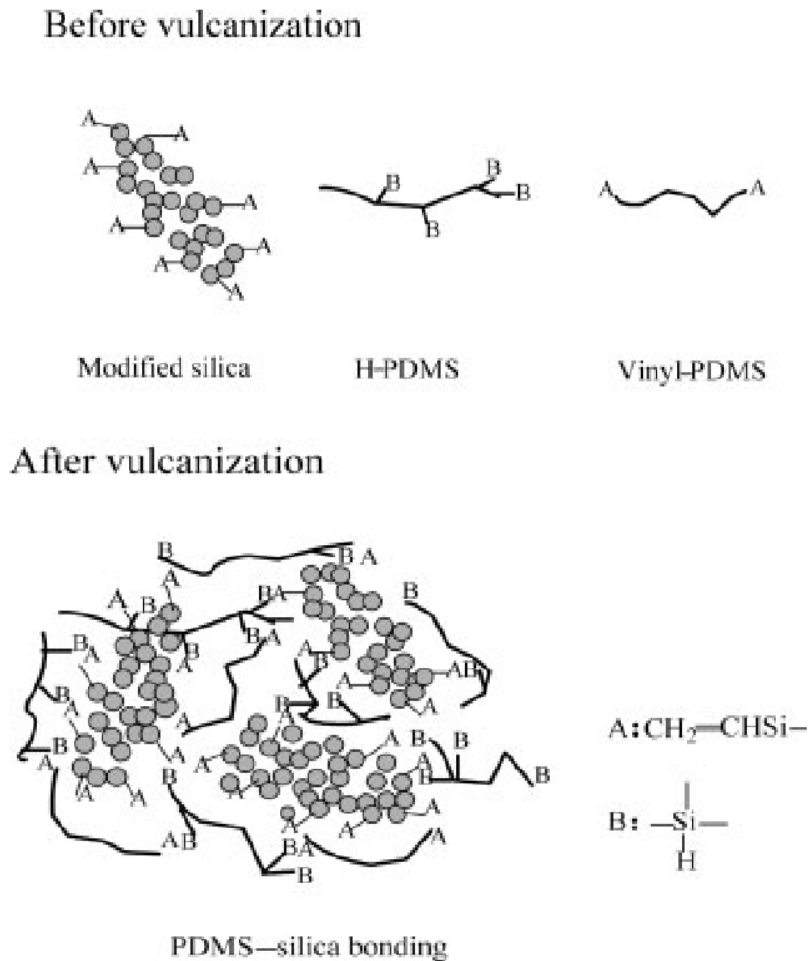


Figure 2.1: Schematic representation of inorganic–organic hybrid network

2.3. Silicone Elastomers in the Industry

Silicone elastomers are elastic substances which contain linear silicone polymers cross-linked in a 3-dimensional network. In most cases this network also contains filler which act as a reinforcing agent or as an additive for certain mechanical, chemical, or physical properties. In general silicones (referred as polydimethyl siloxanes previously) are noted for their high thermal stability, biocompatibility, hydrophobic nature, electrical and release properties. When silicones are cross-linked to form a silicone rubber their characteristic properties are still prevalent. Hence silicone elastomers can be widely used in a great variety of applications. Some examples are shown in Table 2.2. The nomenclature classifies silicone elastomers by their curing mechanism and curing conditions, Silicone rubbers are essentially divided into two groups of materials, i.e., room temperature vulcanizing (RTV) and high temperature vulcanizing (HTV). RTV systems are able to cure at

room temperature and HTV systems at temperatures well above 100°C. A number in the name indicates the number of components that upon mixing will form a curable composition, e.g., RTV-2.

Table 2.2: Brief Overview of Applications for Silicone Elastomers

Application Area	Applications
Automotive	Exhaust pipe hangers Crank shaft seals Radiator seals Ignition cables Connector Seals Spark plug boots
Medical	Catheters Respiration masks Various valves (e.g., dialysis apparatus) Anaesthetic tubing (composite) Body contact electrodes X-ray opaque shunts Various pads
Wire and Cable	Wear resistant cables Instrument cables Safety signal cables Safety power cables Battery cables Economy grade cables Heat resistant cables

Table 2.2: Brief Overview of Applications for Silicone Elastomers *continued*

Sanitary and Household	Gaskets in tap water equipment Gaskets for toilets O-rings (composite) Various valves
Transmission and distribution (T&D) Electronics	Medium and high voltage insulators Medium and high voltage cable accessories Anode caps and cables Key pads (composite) Various gaskets Encapsulation Coatings Adhesives Pottings
Food appliances	Food dispensing valves Various gaskets Baby care articles
Mouldmaking	Prototyping Models for design and/or display Functional models Pre-series models Working moulds for gypsum Plaster moulding Ornaments and window frames Moulded furniture parts Imitation leather moulds Moulds for shaped foodstuffs (e.g., chocolate) Do-it-yourself (DIY) applications Archeological applications

HTV rubbers are mainly so-called solid silicone rubbers. They have a very high viscosity in the uncured state and appear as solids. This behavior has also led to the creation of the term ‘High Consistency Rubber’ (HCR).

Approximately 25 years ago a new group of materials appeared that was intended for processing in injection moulding machines. Because of their low viscosity and paste-like behavior they were named liquid silicone rubbers (LSR) or simply liquid rubbers (LR). It is common to use LSR or LR as an abbreviation instead of HTV, even though they vulcanize at high temperatures as in the case of solid silicone rubbers.

For the most part all LR materials are 2 component systems which cure after mixing and at elevated temperatures.

In summary the silicone industry uses the terms RTV- 1, RTV-2, LR or LSR, HTV or HCR. These refer to the material categories as follows:

RTV-1 Room temperature vulcanizing, one-component

RTV-2 Room temperature vulcanizing, two-component

HTV High temperature vulcanizing, solid silicone rubber, high consistency rubber

LR Liquid rubber, liquid silicone rubber (which is also cured at high temperatures)

In 1999 the global market consumed approximately 170,000 tons of silicone elastomers.

Below figure shows the market shares between the material categories. Among all silicone elastomers LR exhibits the highest growth rate and HTV has the highest portion of the market.

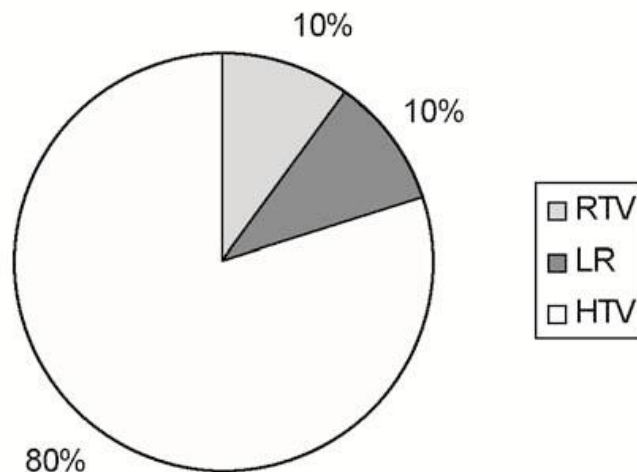


Figure 2.2: Silicone elastomers world market by material categories

The specific requirements of car builders and their system suppliers have made silicone elastomers an indispensable raw material for automotive components. One should also mention that silicone fluids, fumed silica, tire release agents, paint additives, silicone polish and resins are as indispensable for car components as silicone elastomers. The key reasons for the consumption of silicones in automotive applications are numerous. Heat resistance, cold flexibility, oil and chemical resistance mainly account for the use of silicones in the engine and areas close to the engine. Long-term properties such as 'infinite' flexibility and low compression set make silicones the perfect choice for airbag coatings, gaskets, bellows, profiles, etc. Very high dielectric strength and surface resistance, and hydrophobic behavior are required in electric installations for cars. This, however, holds for most wire and cable applications. Apart from being 'perfect' electrical insulators, silicone elastomers can be modified to become electrically conductive parts which are then used, for example, in parts for the ignition system (such as the ignition cable inner lead and spark plugs). The dielectric and other properties make them suitable for spark plug boots and encapsulation of electronic components (even safety components such as airbag and ABS controls). Any application related to the car body is subjected to most of the property requirements already mentioned. UV stability is another predominant requirement for parts used in such applications. The term 'stability' means that a material will not immediately or slowly change its properties over time on exposure to a certain condition. In other words, a given mechanical and/or chemical parameter should change as little as possible. In most cases specifications include relative changes over time (changes in percentage of a property value compared to the initial values).

The field of applications for silicone elastomers is as wide in medical applications as in the automotive sector. Furthermore this is a growing sector, because of the substitution of other organic elastomers, such as latex, and thermoplastics, such as PVC. Reportedly silicone elastomers have often been discussed as the ideal material for medical devices and applications. This also includes the genetics, biotechnology and pharmaceutical industries. The main reason for this great interest in silicone rubber is due to its biocompatibility. For example, silicone rubbers show:

NO pyrogenicity (NO body temperature reaction),
NO hemolysis (NO red blood cell destruction) and
NO cytotoxicity (do not affect live cells).

The key reasons for the consumption of silicones in medical/pharmaceutical devices and equipment are: biocompatibility, gamma ray resistance, chemical resistance, sterilisability (gamma ray, ethylene oxide (EtO), steam), pigmentability, transparency, durability, and the fact that they are non-allergenic. In addition, all the properties mentioned under the automotive section also complement their competitive advantages compared to other organic elastomers. As many medical devices must be manufactured under special hygienic conditions, in compliance with Good Manufacturing Practice (GMP), in cleanrooms, silicones seem to be a good choice of materials as well. In many cases they can be processed almost without forming any reaction products, which might impair purity, smell or sterility of the manufactured goods. Silicones are not only bio inert, their excellent electrical insulating properties make them a useful component of any medical equipment, be it sensoric, or for resuscitation, etc. This is also supported by their hydrophobic behavior, which prevents them from accumulating moisture from the surrounding environment.

Summing up we can draw the conclusion that silicones have a great future in medical device technology. However, their reputation as long-term implants has been sullied after the bad press and the vast number of lawsuits with respect to silicone breast implants. In order to support the duty of care of suppliers to the medical device industry, in most cases silicone manufacturers have set internal healthcare guidelines. Basically this list allowed applications for each material and those that are not supported by the silicone manufacturer. As a general rule, many silicone manufacturers restrict their supply to this industry to short-term implants. In other words, the providers of silicone elastomers will not usually support implants or devices involving permanent body contact (longer than 29 days).

CHAPTER 3

3. Experimental

This chapter contains experimental processes used in this thesis work. This part covers perlite preparation and characterization (Titration, X-Ray Diffraction - XRD, BET surface analysis, Scanning Electron Microscopy - SEM, pycnometer analysis), attrition milling and characterization of nano-perlite (Dynamic Light Scattering – DLS), experimental studies in perlite expansion and characterization (Hot Stage Microscopy, SEM, pycnometer analysis), surface modification of nano-perlite and finally masterbatch preparation using PDMS and nano-perlite, cured elastomer characterization (Universal Testing Machine – UTM, Rheometer).

3.1. Perlite Preparation

All of perlite used in the characterization experiments and attrition milling experiments is industrial, which means processed in vertical expansion furnaces, therefore called expanded perlite.

3.1.1. Ball Milling

It has been observed in prior experimental studies that industrial perlite contains some contamination. In order to eliminate this problem, expanded perlite has been ball milled first to obtain a fine powder. In this method, ceramic balls which are 50 grams in mass were filled into 10 liter plastic drums. Then, expanded perlite was added into the drums which were then placed on a double-band process mill, rotating the drums horizontally around their own axes for 24 hours. Due to rotation around horizontal axis and internal cascading effect, ceramic balls have modified expanded perlite into fine ground powder.



Figure 3.1: Ball Milling Process

3.1.2. Screening

After ball milling, expanded perlite was screened in order to clear contamination from the material. Sieves with mesh sizes 25 μm , 43 μm , 102 μm and 182 μm were placed on top of each other and were applied vibration. Perlite was then poured on the top mesh (182 μm in size). After 30 minutes of vibration, perlite was cleared from all of the contamination, which could not go past the top of the setup.

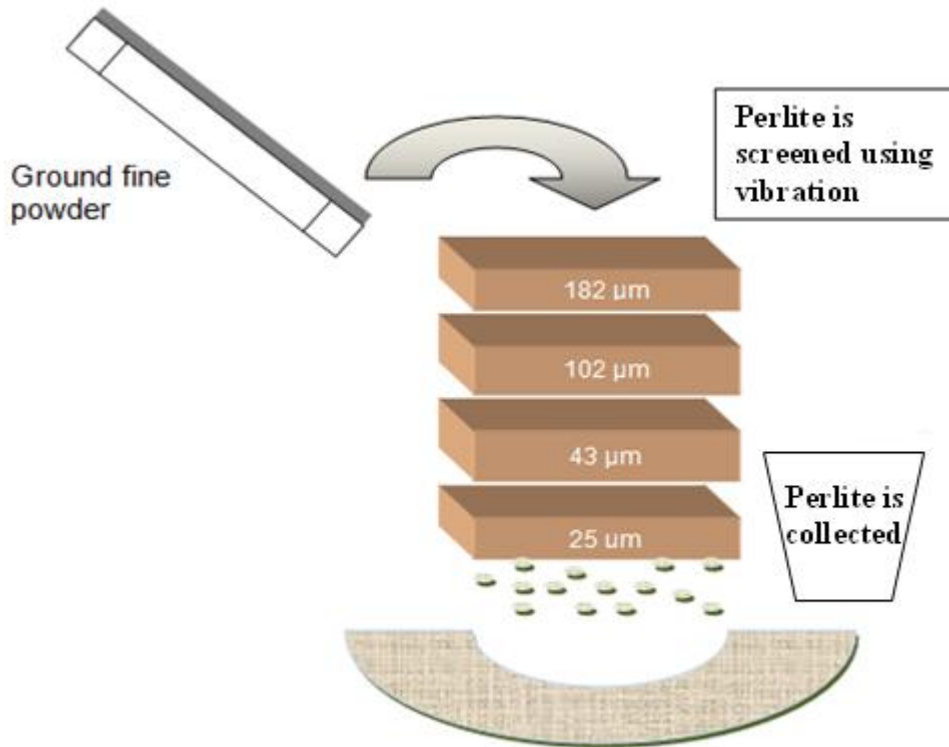


Figure 3.2: Setup used to screen perlite using vibration

3.2. Perlite Characterization Experiments

3.2.1. Surface Titration

Surface titration experiment was carried out to determine hydroxyl ($-\text{OH}$) group density on perlite surface. This is crucial as it is important to know if there is an adequate number of functional groups on the mineral surface to undergo chemical reaction which might be necessary to increase interaction between perlite particles and PDMS. Therefore, the below procedure is used to calculate surface hydroxyl group number per a gram of perlite:

- 0.05 M NaOH is added to 2 grams (W) of perlite and they are mixed for 12 hours;

- 10 ml is taken from the centrifuged mixture;
- 0.05 M HCl is used to neutralize the 10 ml solution. A ml of HCl is used;
- B ml of 0.05 M HCl is used to neutralize 0.05 M NaOH (without perlite added);
- Therefore, X is the amount of surface OH groups per unit weight, using the below formula:

$$X = \frac{(B - A) \times 0.05 \times 8}{W}$$

3.2.2. X-ray Diffraction Measurements (XRD)

X-ray diffraction patterns were recorded with a Bruker AXS advance powder diffractometer equipped with a Siemens X-ray gun and Bruker AXS Diffrac PLUS software, using Cu Ka radiation ($k = 1.5418$ Angstrom). All samples were scanned from $2\theta = 2^\circ$ to 10° and $2\theta = 10^\circ$ to 90° .

3.2.3. Pycnometer Analysis

Density of expanded perlite was determined using a Quantachrome Automatic Gas Pycnometer for True Density Ultrapyc 1200e using standard sample cell with 10 cm^3 nominal volume, 24 mm internal diameter and 23 mm internal depth.

3.2.4. BET Surface Analysis Test

Specific surface area was determined by Quantachrome NOVA Surface Area Analyzer with nitrogen and methane. BET Surface Analyzer has a fully automatic microbalance system that allows measuring weight change as a function of time, gas pressure and the sample temperature. The precision of the measurement can be controlled by a PC. Long term stability of microbalance is $0.1 \mu\text{g}$ with a weighting resolution of $0.2 \mu\text{g}$ and temperature stability is 0.1°C .

3.2.5. Scanning Electron Microscopy (SEM)

Morphological characterization of samples were performed using the a Gemini scanning electron microscope equipped with Leo 32 Supra 35VP field emission scanning system and electron dispersive spectrometer. An accelerating voltage between 2-5 kV was used during the measurements.

3.3. Nano-Perlite Production Using Attrition Milling and Its Characterization

Expanded perlite and unexpanded (raw) perlite were attrition milled separately for further studies. Attrition milling was done inside a Draiswerke Bead Mill DCP with grinding media of zirconium beads 0.3 mm in size, agitator arm at 1800 rpm.

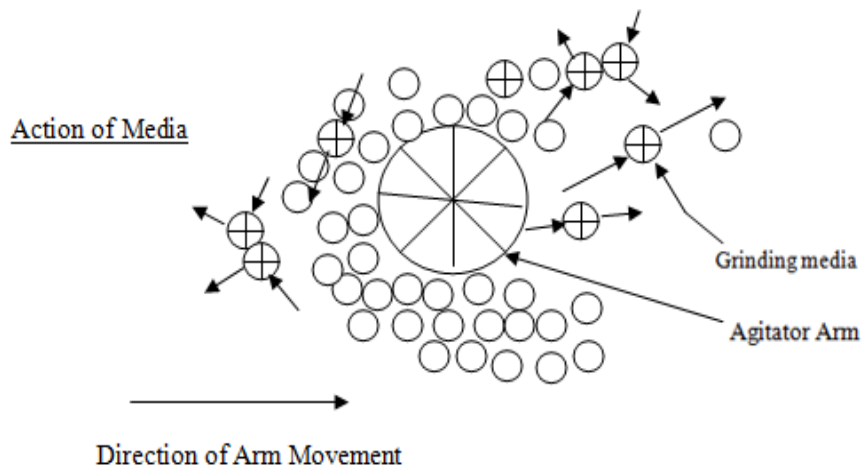


Figure 3.3: Working Principle of Attrition Mill

Some parameters concerning the output of the Attrition Mill were considered before experiments. Below is the list and explanation of the parameters that were deliberated in order to reach smallest particle size for perlite samples:

Rotation speed: Agitator arm speed can be adjusted between 0-1800 rpm. As the rotation speed increases, particle size will decrease. In the experiments performed in thesis work, agitator arm speed was set at 1800 rpm to obtain the smallest particle size available.

Feeding rate: As rate of feeding material to the grinding environment decreases, particle size decreases. This rate can be varied using the speed button on the peristaltic pump.

Bead size: As the bead size decreases, smaller particles can be obtained; however in trial experiments it was seen that 0.1 mm beads caused a blockage in the filter inside the Attrition Mill. Therefore, 0.3mm beads were used.

Time: Particle size depends on run time too. As run time of milling increases, smaller particles are obtained.

Suspension concentration: In order to avoid blockage of the hoses that provide circulation between the Attrition Mill and the peristaltic pump, perlite concentration was kept at 20 %.

The following schematic summarizes the steps that were done in order to produce adequate amount of nano-perlite to use in masterbatch preparation:

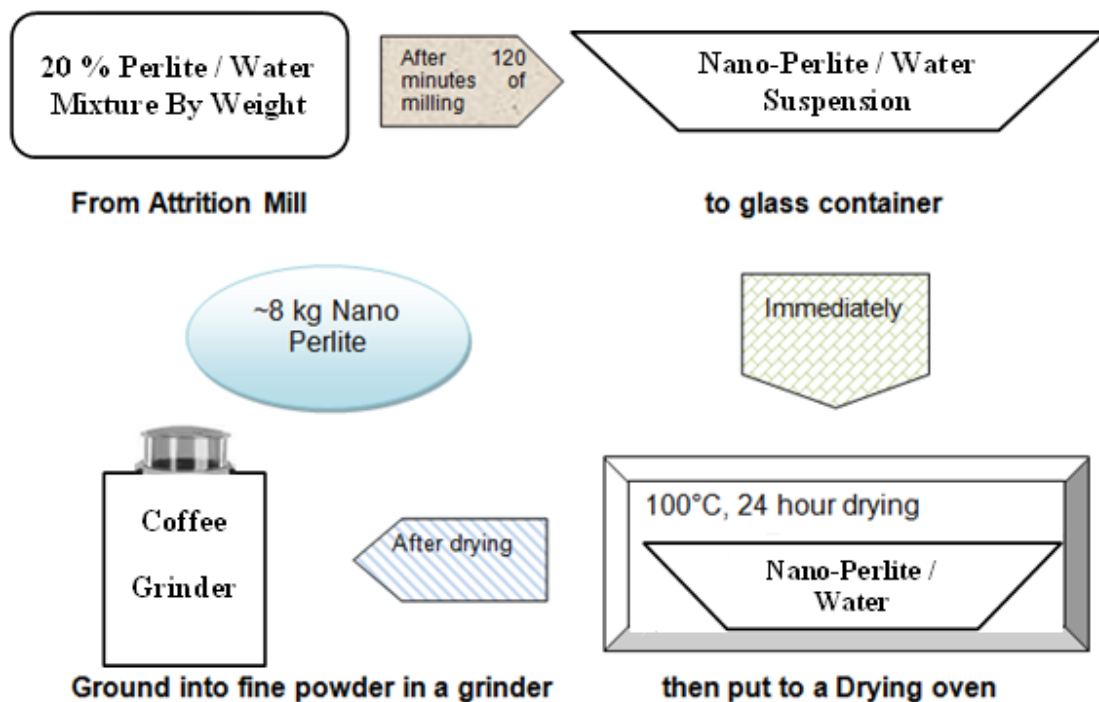


Figure 3.4: Nano-Perlite Production Scheme

3.3.1. Dynamic Light Scattering Measurements (DLS)

Dynamic Light Scattering measurements were recorded with a Malvern Zetasizer Nano-ZS, using disposable cuvettes to measure 3 different runs with 10 repeats in each run.

3.3.2. SEM Analysis

Morphological characterization of nano perlite was done using the a Gemini scanning electron microscope equipped with Leo 32 Supra 35VP field emission scanning system and electron dispersive spectrometer. An accelerating voltage between 2-5 kV was used during the measurements.

3.4. Perlite Expansion Experiments

In order to study the expansion character of raw perlite, experiments were carried out in laboratory conditions.

3.4.1. Expansion

Raw perlite was heat treated in Nüve MF 106 high heat furnace at various temperatures. Samples were placed inside ceramic crucibles able to withstand high temperature without deformation.

3.4.2. Hot Stage Microscopy Experiment

Hot Stage Microscopy measurements were recorded at Esan Eczacıbaşı's laboratories in Hot Stage Microscope Misura ver. 3.32 between 22°C and 1365°C.

3.4.3. Pycnometer Analysis

Density of heat treated perlite was determined using a Quantachrome Automatic Gas Pycnometer for True Density Ultrapyc 1200e using standard sample cell with 10 cm³ nominal volume, 24 mm internal diameter and 23 mm internal depth.

3.5. Surface Modification of Nano-Perlite and its Characterization

To increase its compatibility with silicone, nano-perlite surface was modified using Hexamethyldisilazane. The following schematic summarized the steps that were done in order to achieve previously stated goal:

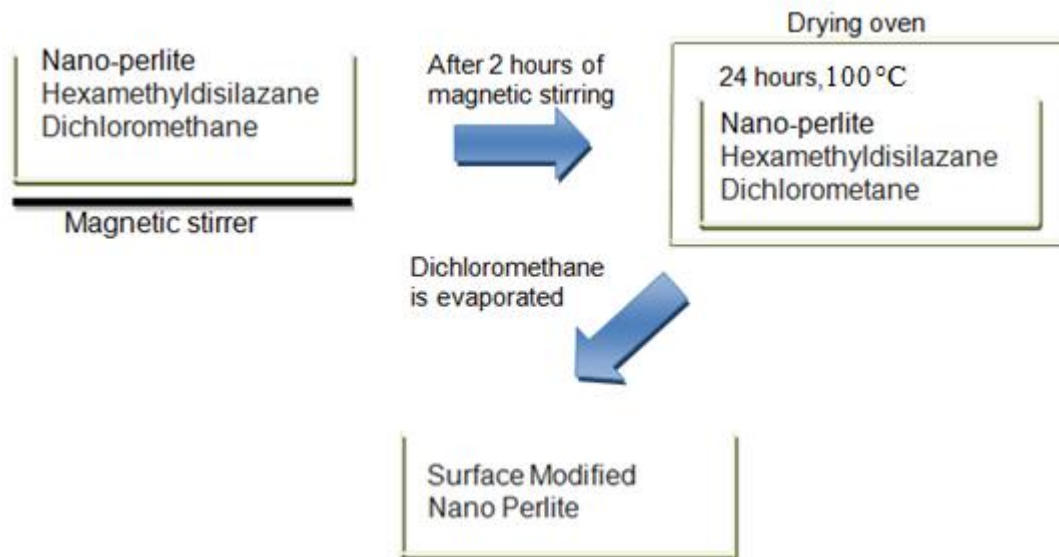


Figure 3.5: Nano Perlite Surface Modification Procedure

3.5.1. Separating Nano-Perlite from Suspension

Nano-perlite - water suspension was put inside a drying oven, and left for 24 hours at 100°C. After 24 hours, perlite was recovered from a glass container.

3.5.2. Grinding Nano-Perlite into Fine Powder

In order to incorporate nano-perlite into silicone, it was essential that nano-perlite was in the form of a fine powder. Therefore, nano-perlite after it was collected from drying oven was placed inside a Krups GVX2 Grinder and was ground until it was ready to mix.

3.5.3. FT-IR Analysis

FT-IR analyses of the samples have been conducted by using Thermo Scientific - Nicolet IS10 FTIR with KBR transmittance accessory. KBR pellets were prepared 1/100 sample ratio at 9 ton pressure.

3.5.4. Thermogravimetric (TGA) Analysis

TGA analyses of the samples have been conducted by using NETZSCH STA 449C Simultaneous TGA/DTA Analyzer RT-1500°C.

3.6. Masterbatch Preparation

Nano-perlite and PDMS were mixed inside a Linden Maschinenfabrik 10 lt. butterfly mixer, connected to vacuum and nitrogen. Below is the schematic of the mixing procedure illustrating the mixer and process:

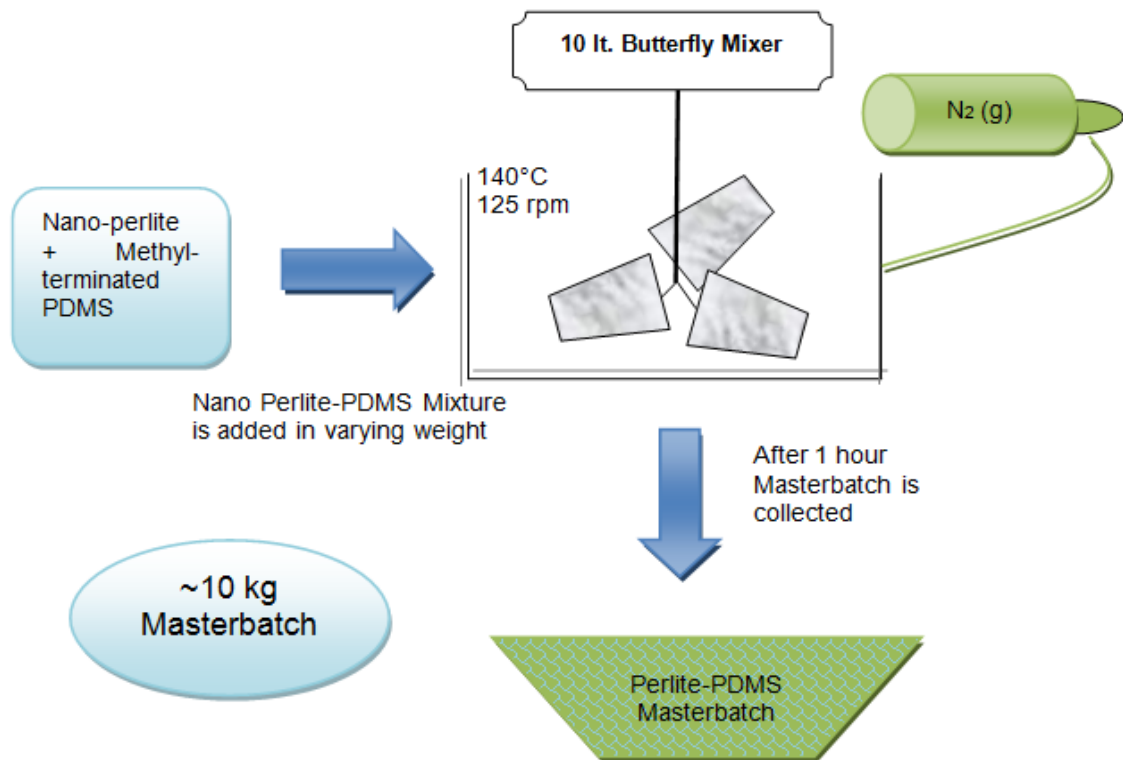


Figure 3.6: Nano Perlite-PDMS Masterbatch Preparation

3.7. Cured Elastomer Characterization

Nano-perlite and PDMS were mixed to obtain Masterbatches with various filler loading levels. Masterbatches were then used to prepare cured elastomer formulations.

3.7.1. UTM Analyses

After cured elastomer formulations were prepared, they are tested for their mechanical properties (tensile strength, elongation at break, tear strength) using Instron 3345 Testing System. Hardness measurements were done using a Zwick Shoremeter.

3.7.2. Rheology Analyses

Rheology studies were recorded using Dynisco RPA 2000 in frequency sweep mode using 1°C stress angle.

CHAPTER 4

4. Results and Discussion

4.1. Raw Perlite Preparation, Characterization, Expansion

In this chapter, results of experimental studies regarding raw, expanded and surface treated perlite characterization results before and after attrition milling will be presented and discussed. These experiments are: surface titration, X-Ray Diffraction - XRD, BET surface analysis, Scanning Electron Microscopy - SEM, pycnometer analysis and Dynamic Light Scattering – DLS.

In order to proceed with perlite studies, raw perlite was chosen as the reference point and results obtained from its characterization were used to direct this research in the right way.

4.1.1. Raw Perlite Preparation

Ball Milling

Water is used as carrier medium in attrition milling, and its purpose is to transfer material to be grounded from the feeding unit to the grinding environment and vice versa. When raw perlite is placed in water, due its hydrophilic structure, it attracts water inside its pores which then causes a huge decrease in the fluidity of the system. Because of this fluidity decrease, when perlite-water concentration is more than 5% hoses providing circulation between the mill itself and the peristaltic pump (which is utilized for feeding and circulation purposes) are blocked. Due to this reason, raw perlite has been ball milled to make it smaller in particle size and eliminate its porous structure; which in turn has resulted with an ability to feed concentrations of 20% without any trouble. In ball milling method, ceramic balls rotate in horizontal axis for 24 hours inside a plastic drum along with expanded perlite, as explained in 3.1.1. Using this method, raw perlite which was millimeters in size has been reduced to a fine powder ready to be used.

Screening

In preliminary studies with the Attrition Mill in lab premises, it has been observed that after raw perlite was ball milled and fed in the mill, certain substance inside perlite has not been milled and resulted in contamination in final output. Therefore,

raw perlite that was ball milled was further processed to eliminate this contamination by being screened through 4 sifts which are 25 μm , 43 μm , 102 μm and 182 μm in mesh size. A vibrating motor was placed on bottom of sifts which were sitting on top of each other, with 182 μm on very top. Perlite was poured on top and 30 minutes of vibration was applied, this resulted in contamination being cleared from the fine powder.

4.1.2. Raw Perlite Characterization

4.1.2.1. XRD Analysis

X-Ray Diffraction technique was employed to determine the crystal structure of expanded perlite. As it can be seen in figures 4.1, (1-10 microns) there are no crystal peaks observed in the XRD spectra of raw perlite in this particle size. This result confirms that the mineral has no crystal structure just like amorphous silica.

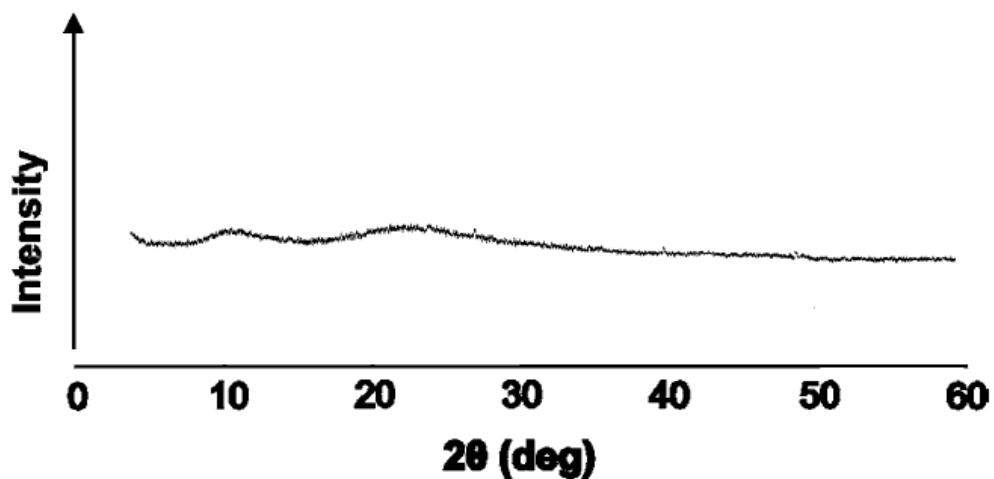


Figure 4.1: XRD Spectrum of Raw Perlite (Particle size between 1-10 microns)

4.1.2.2. BET Surface Analysis

Using BET Surface Analyzer in laboratory premises, the specific surface area of raw perlite was calculated to be $1.9 \text{ m}^2/\text{g}$.

4.1.2.3. Pycnometer Analysis

At 20°C , density of raw perlite was calculated to be $2.3 \text{ gram}/\text{cm}^3$. Density of amorphous silica at this temperature is around $2.2 \text{ gram}/\text{cm}^3$. This result shows that perlite has a similar density compared to silica.

4.1.2.4. SEM Characterization

Scanning Electron Microscopy was used to analyze particle size and structure of raw perlite was studied. Raw perlite structure can be seen in the below SEM image. The wide size distribution of perlite particles can be observed, which is parallel to the Dynamic Light Scattering results.

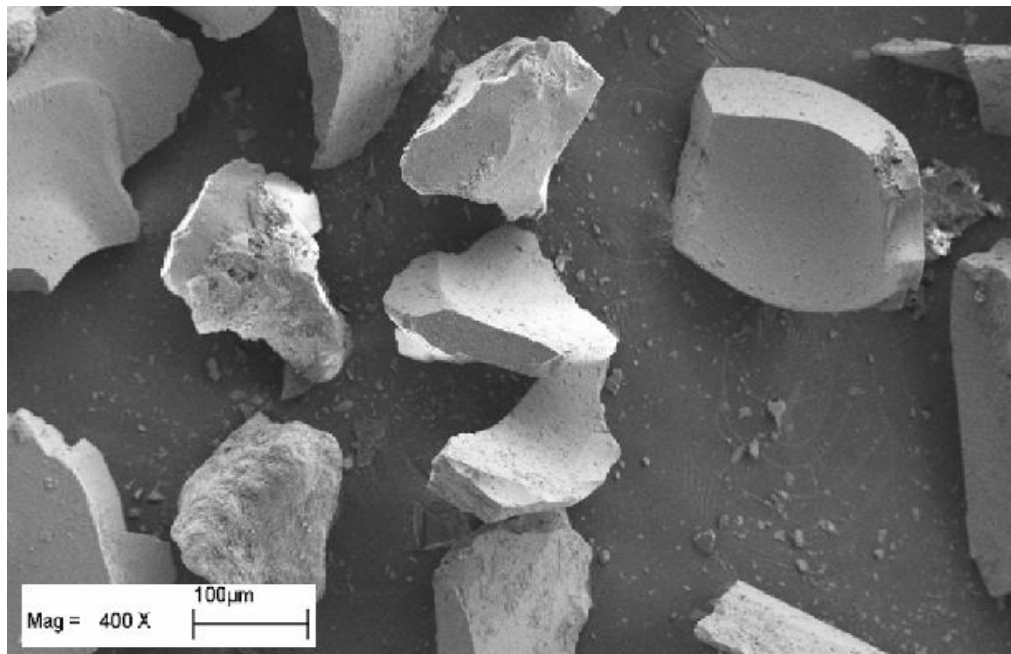


Figure 4.3: Raw Perlite Particle at 4000 magnification

4.1.3. Raw Perlite Expansion and Characterization

Prior to expansion studies of raw perlite, it has been ball milled and sifted. This was done in order to improve attrition milling process of the material and therefore attain smaller particle size.

4.1.3.1. Expansion Using Laboratory Furnace

In order to understand the expansion character of raw perlite and draw conclusions, perlite samples were prepared to be heat-treated at 870°C (since this is the critical temperature at which it expands) for 10 seconds, 30 seconds, 1 minute, 2, minutes, 5 minutes, 10 minutes and 30 minutes.

4.1.3.2. SEM Analysis of Perlite Particles

From Figure 4.4 to 4.10, the change of heat processed perlite as a function of time can be seen.

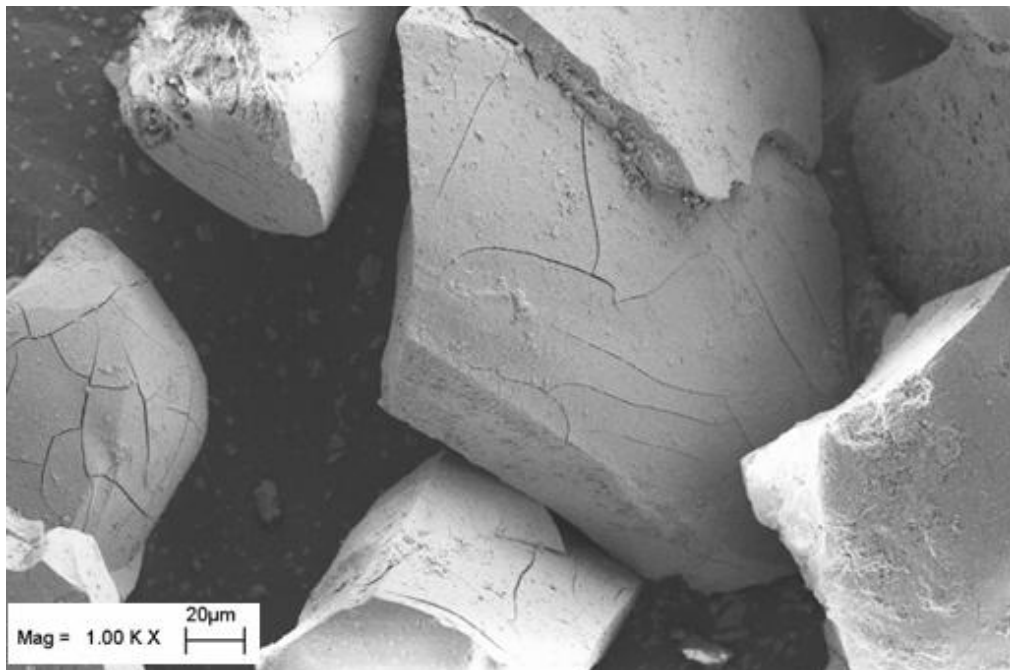


Figure 4.4: Raw Perlite (After 10 seconds)

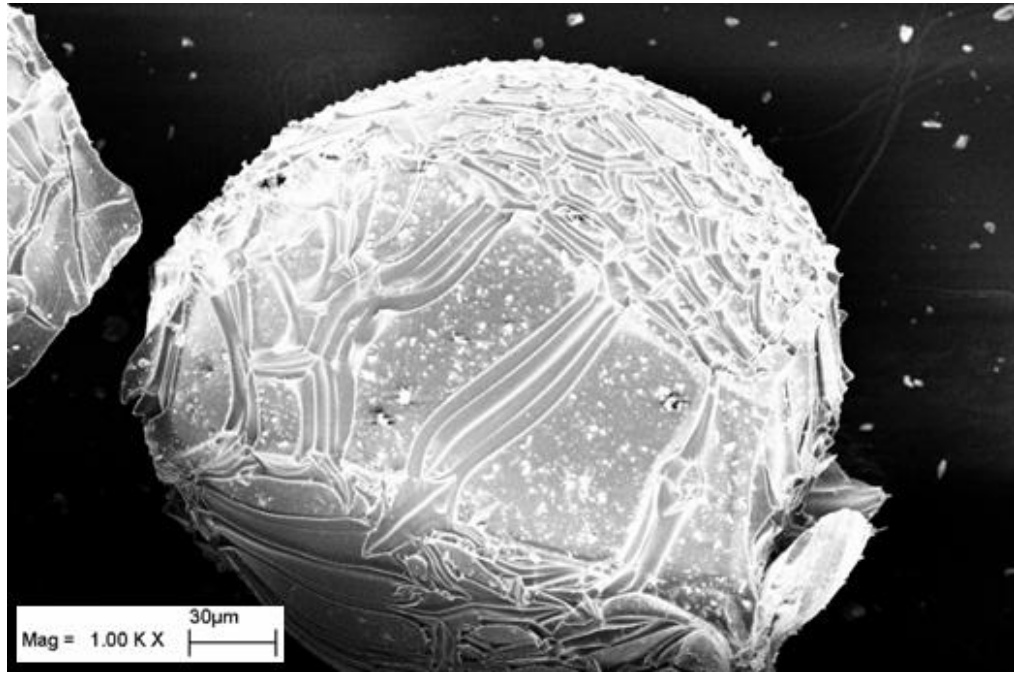


Figure 4.5: Raw Perlite (After 1 minute)

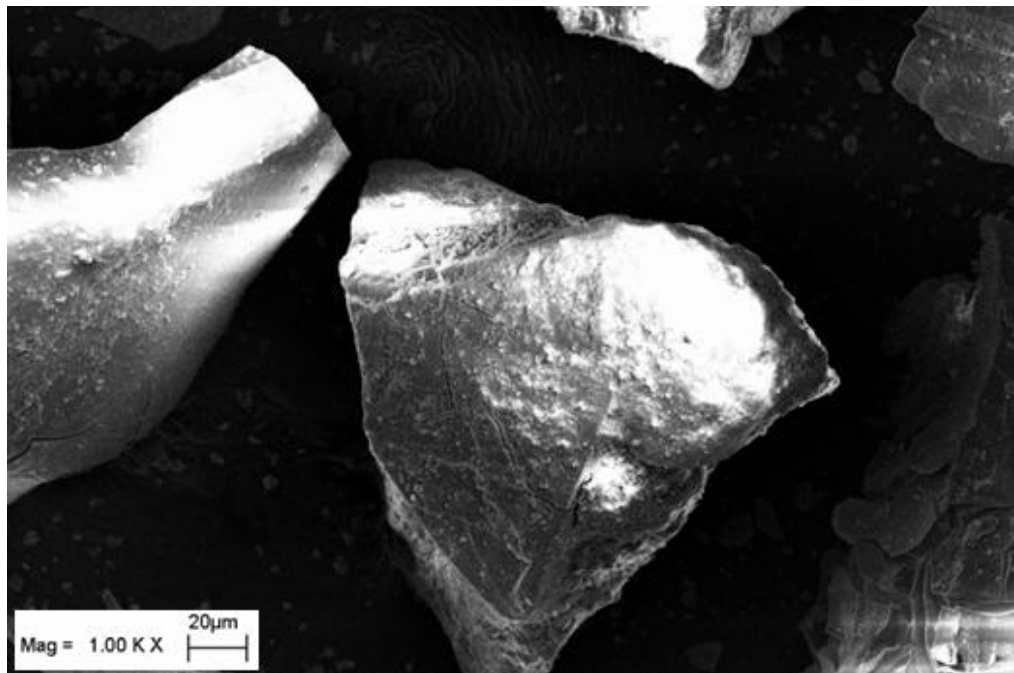


Figure 4.6: Raw Perlite (After 2 minutes)

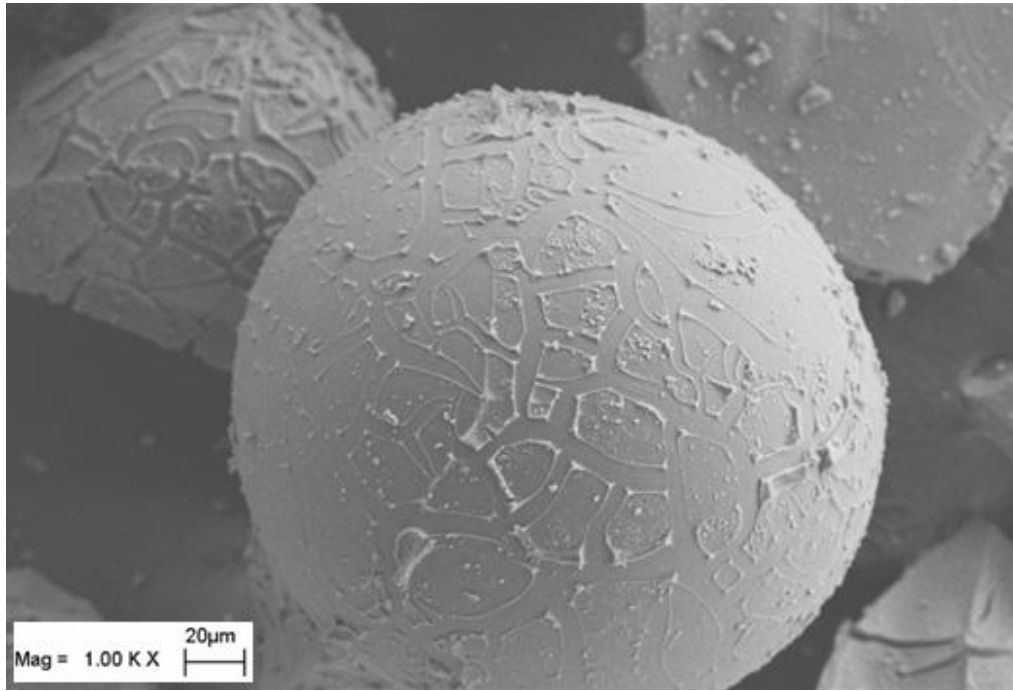


Figure 4.7: Raw Perlite (After 10 minutes)

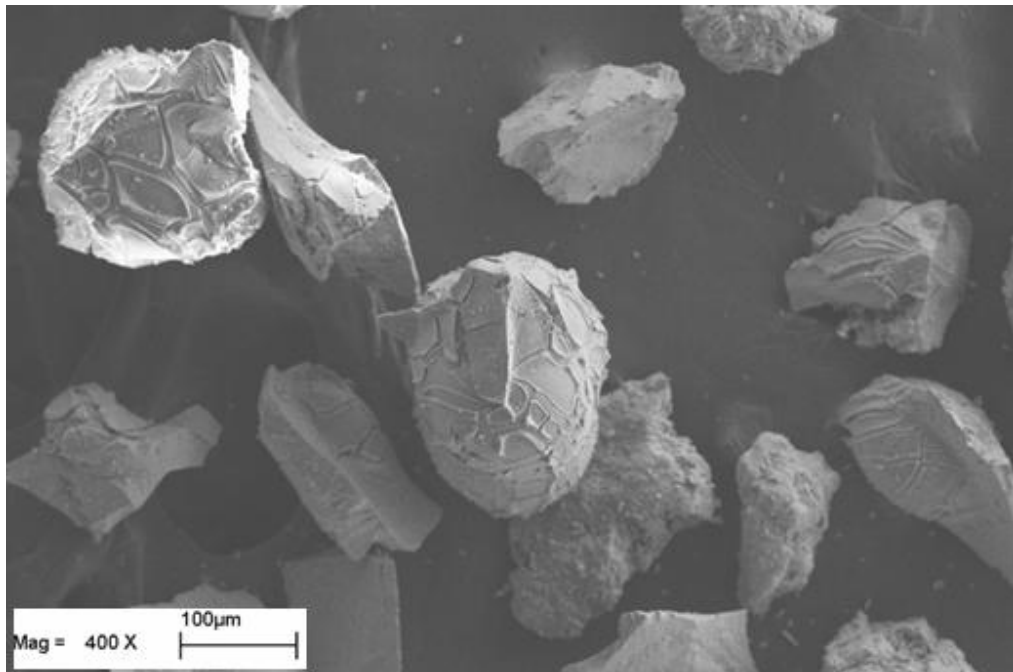


Figure 4.8: Raw Perlite (After 10 minutes)

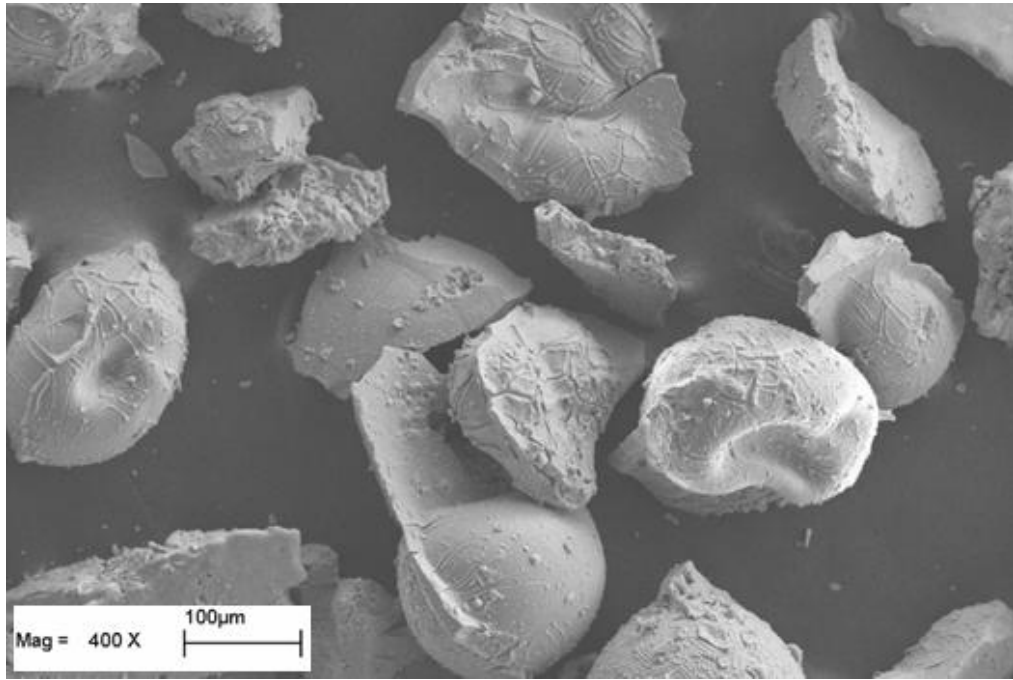


Figure 4.9: Raw Perlite (After 30 minutes)

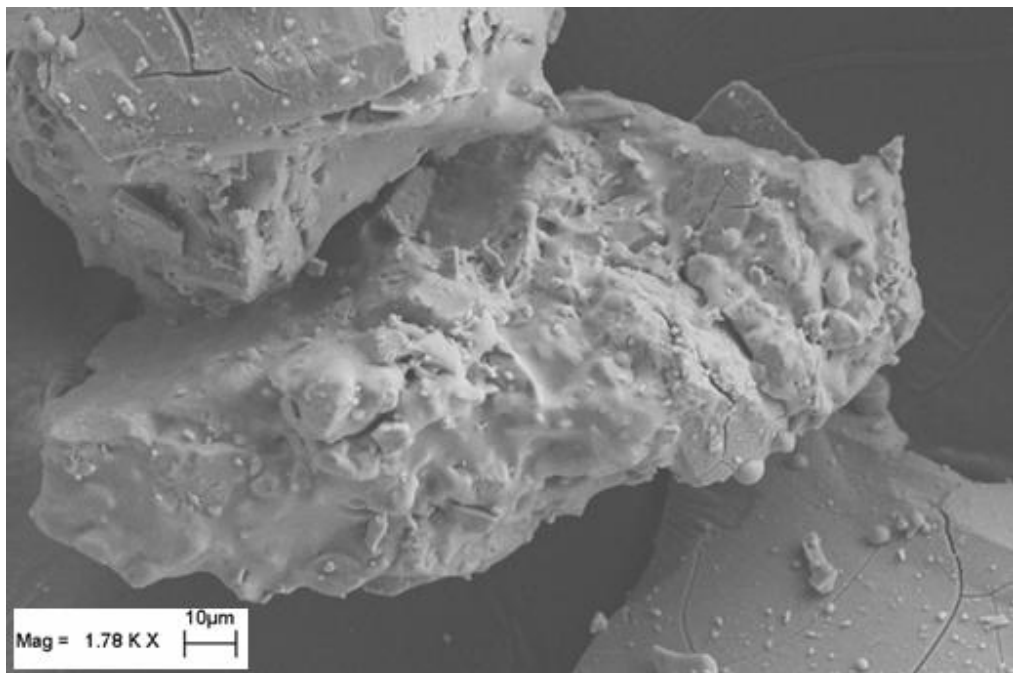


Figure 4.10: Raw Perlite (After 30 minutes)

As it can be seen in the above images, perlite particles which have not been ground are applied heat and they start only to swell. As a result, a possible conclusion was that if

perlite particles size was reduced to nano-scale using attrition milling method and then applied heat, expansion would be observed instead of only swelling.

After heat treatment of unexpanded and unground perlite, it can be seen that there is no significant change in particle size. Heat treatment process is open for debate, however it is a possibility that inside the perlite particles, porous configurations would form.

4.2. Nano Raw Perlite Preparation, Characterization, Expansion and Elastomer Preparation

4.2.1. Nano Raw Perlite Preparation and Characterization

4.2.1.1. Attrition Mill Process

Since the main goal in using the Attrition Mill was to reduce particle size of raw and expanded perlite to the nano scale, Attrition Mill parameters were thoroughly considered and an optimization study was designed using these said parameters:

Rotation speed: Agitator arm speed was adjusted to 1800 rpm to get the smallest particle size.

Feeding rate: The feeding was adjusted to 2; 1 being slowest and 5 being fastest. 2 was chosen as to keep perlite particles longer in the grinding environment and to avoid hose blockage in the system as speed 1 triggered some problems earlier in the experiments.

Bead size: In trial experiments it was seen that 0.1 mm beads caused a blockage in the filter inside the Attrition Mill. Therefore, 0.3mm beads were used.

Suspension concentration: In order to avoid blockage of the hoses that provide circulation between the Attrition Mill and the peristaltic pump, perlite concentration was kept at 20 %.

Time: Particle size depends on run time too. As run time of milling increases, smaller particles are obtained. In the optimization study, time was the sole factor that was studied closely, keeping every other parameter constant.

4.2.1.2. Optimization Study & Dynamic Light Scattering

In attrition milling experiments raw perlite has been processed to produce nano particles. Since it was realized that for further investigations there would be need of nano perlite, 8 kilograms of production was targeted. Considering that a single batch takes 90 minutes of production time and that it weighs 150 grams, approximately 60 hours have been spent to milling raw perlite.

Milling Time (minutes)	Particle Size (nm)
5	360
15	304
30	284
45	275
60	249
90	238
120	244

Table 4.1: Attrition Mill optimization study recorded at constant feed rate and 1800 rpm. Right column shows Dynamic Light Scattering results. Unit is nanometers.

The average particle size of expanded perlite that was ground using the Attrition Mill was measured using Dynamic Light Scattering – DLS. For these analyses, samples taken from perlite suspension right after the completion of attrition milling were used. Using double distilled water, perlite concentration was decreased to 0.2 gram/milliliter. Considering that agglomeration will increase with the reduced particle size after attrition milling, samples were stirred for 2 hours using a magnetic stirrer and further kept at ultrasonic bath for another 2 hours.

As seen in Table 4.1, up until 90 minutes, as milling time increases, average particle size decreases and later does not change. However when figures 4.8 and 4.9 that show DLS spectra obtained after 90 and 120 minutes of milling are examined, it can be seen that although there is no significant change in average particle size, there is a wider spread of size after 120 minutes of milling time, which suggests that after 120 minutes there are way more bigger and smaller particles in number in the suspension than the one obtained after 90 minutes of milling. This result actually is an indication that agglomeration plays a vital role in particles milled beyond 90 minutes as they are getting smaller until 120 minutes of run time. Although smaller particles exist in suspension obtained after 120 minutes, optimum run time was chosen as 90 minutes. It was observed that according to the optimization study carried out, expanded perlite's average particle size went down to 260 nanometers.

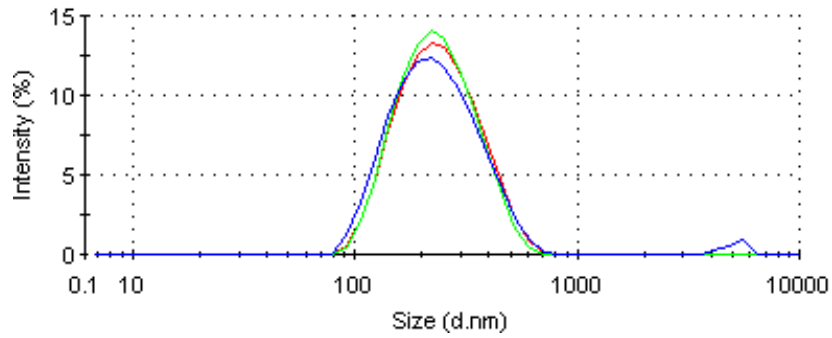


Figure 4.11: DLS Spectrum of Raw Perlite after 60 minutes of Milling

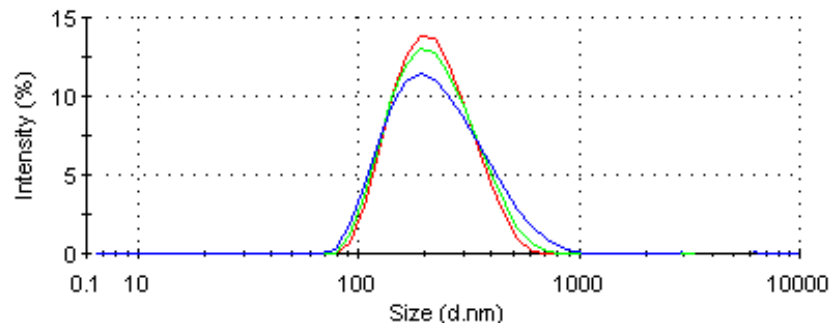


Figure 4.12: DLS Spectrum of Raw Perlite after 90 minutes of Milling

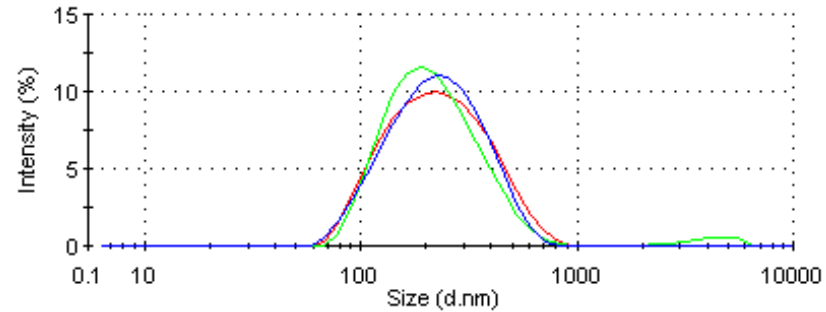


Figure 4.13: DLS Spectrum of Raw Perlite after 120 minutes of Milling

4.2.1.3. BET Surface Analysis

Using BET Surface Analyzer, the specific surface area of nano raw perlite was calculated to be 43.1 m²/g.

4.2.1.4. SEM Characterization

SEM was used to analyze the particle shape of raw nano expanded perlite:

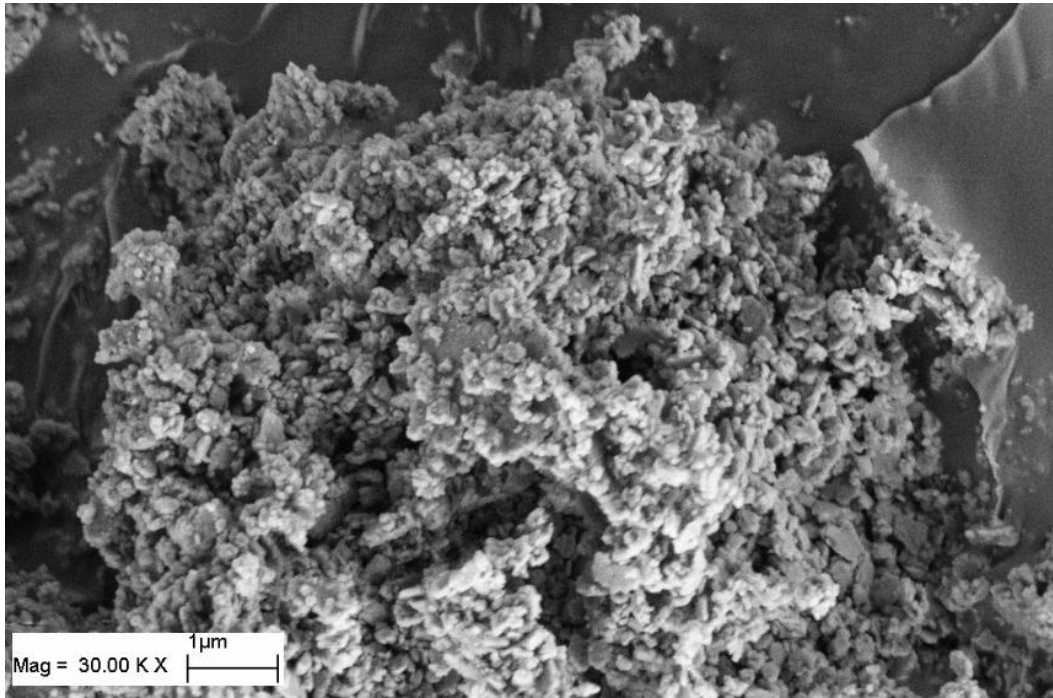


Figure 4.14: SEM Image of Nano Raw Perlite at 30000 Magnification

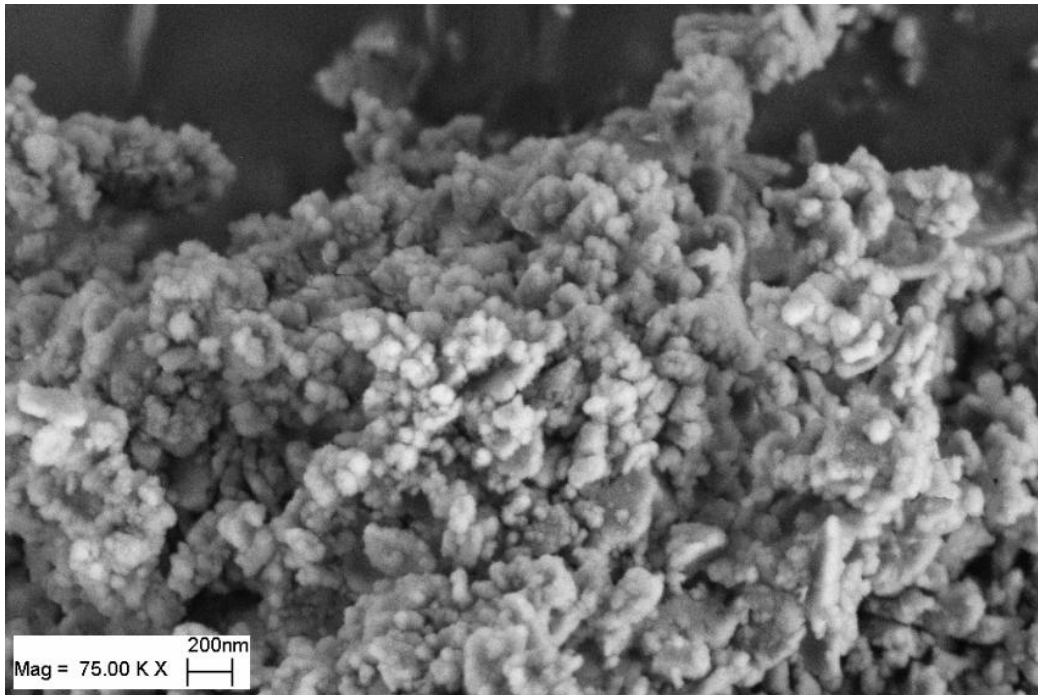


Figure 4.15: SEM Image of Nano Raw Perlite at 75000 Magnification

It can be seen from figure 4.14 that as a result of attrition milling, one of the issues raised beyond the reduction of particle size, is the increase in agglomeration as it

becomes more effective. In figure 4.15, when particles making up agglomerates are closely investigated, it is seen that agglomerates in this image are made up of similar looking platelet shaped nano particles. It is important to note that average particle size is actually smaller than 100 nanometers (around 40-50 nm). One must remember that average particle size subjected to ultrasonic bath was around 400-500 nm. A potential conclusion is that agglomeration becomes increasingly more effective as particle size is decreasing, and that ultrasonic baths are not able to overcome and break agglomerates which results in DLS measurements in an higher average particle size than real size. After attrition milling, the fact that particle size distribution is more homogeneous than in a system not attrition milled, and that particle shape is getting increasingly more spherical are two reasons which might play roles in the observed agglomeration. Above discussion is the reason why further raw perlite expansion study was sparked, because it was thought that more efficient nano structures could be attained if unexpanded perlite was ground and nano-scaled first, and then expanded.

4.2.1.5. Separating Nano Raw Perlite from Suspension

After 90 minutes of processing time in the Attrition Mill perlite suspension was poured in 50 ml falcon tubes, and was applied 30 minutes of centrifugation at 5000 rpm. However, as a result of high centrifugal force perlite was stuck in the bottom of falcon tubes and has become extremely difficult and time consuming to collect. In addition, the fact that water above the settled perlite was cloudy showed that nano raw perlite has not completely settled but that it was still hanging in the water. Therefore, ground perlite suspension was directly put inside a drying oven after attrition milling. Suspension were left to dry for 24 hours at 200°C, and after water has evaporated perlite was placed into an electrical grinder to make it a fine powder.

4.2.2. Nano Raw Perlite Expansion and Characterization

4.2.2.1. Expansion Using Laboratory Furnace

After raw perlite samples from Genper Ltd. have been attrition milled, they have been placed in a laboratory furnace and applied rapid heating at 300, 400, 500, 600, 700 and 800°C for 10 minutes inside ceramic crucibles.

4.2.2.2. SEM Analysis of Perlite Particles

Below are the SEM images of the nano raw perlite samples which have been heat treated:

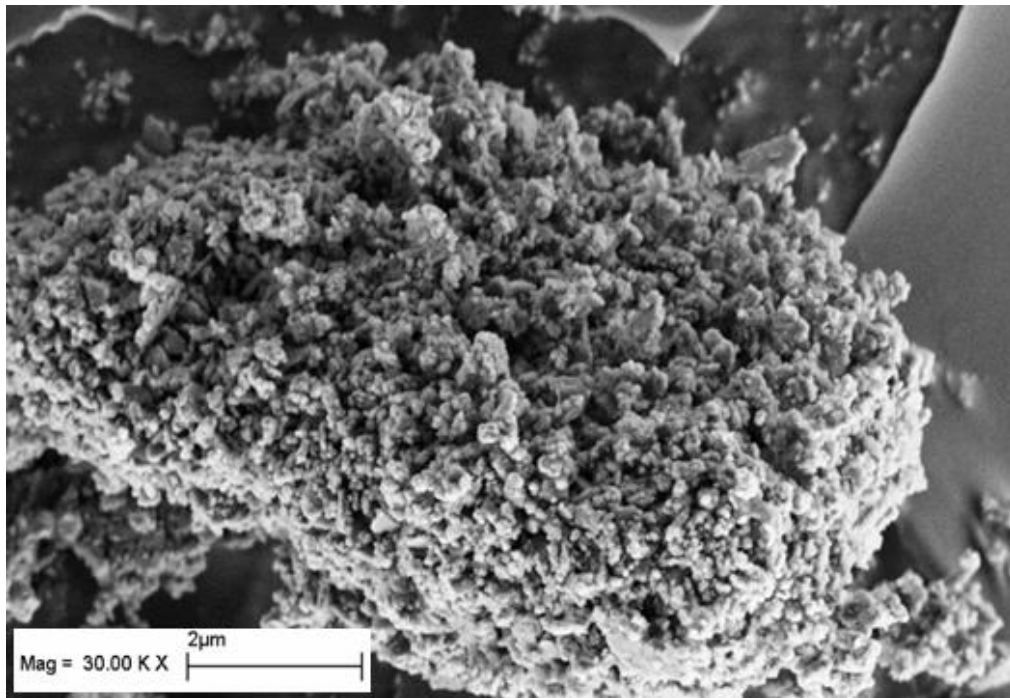


Figure 4.16: SEM Image of Ground Raw Perlite kept at 300°C for 10 minutes, 30000 Magnification

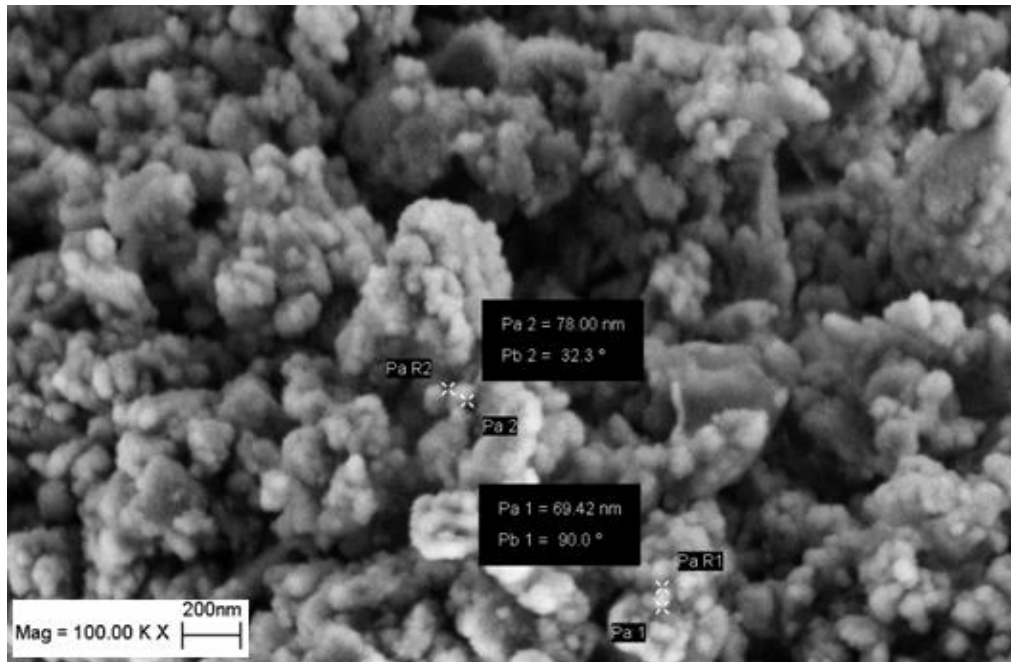


Figure 4.17: SEM Image of Ground Raw Perlite kept at 300°C for 10 minutes, 100000 Magnification

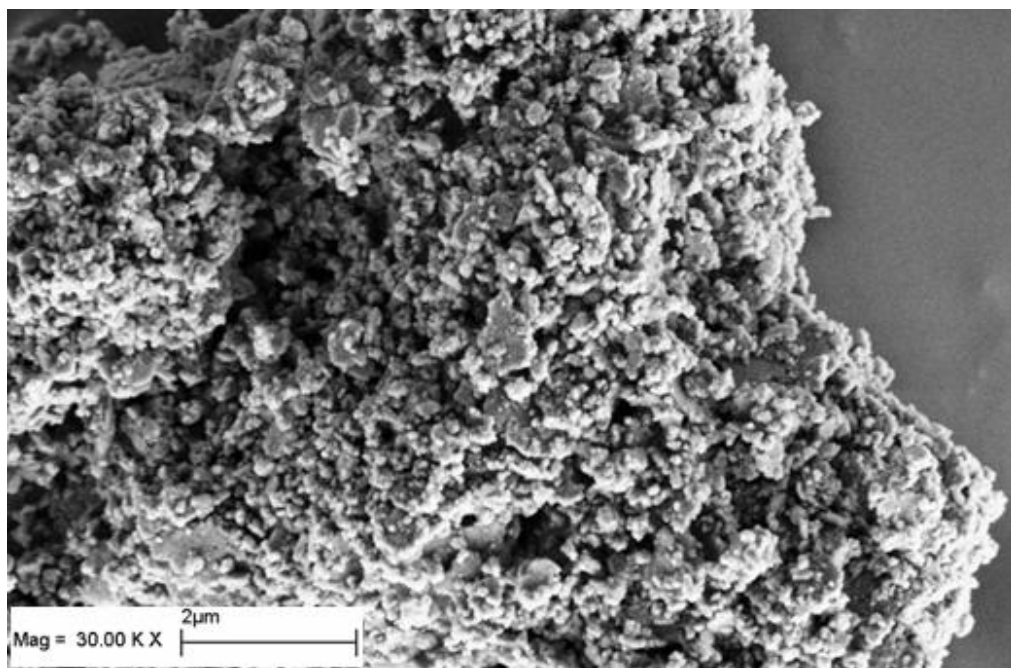


Figure 4.18: SEM Image of Ground Raw Perlite kept at 500°C for 10 minutes, 30000 Magnification

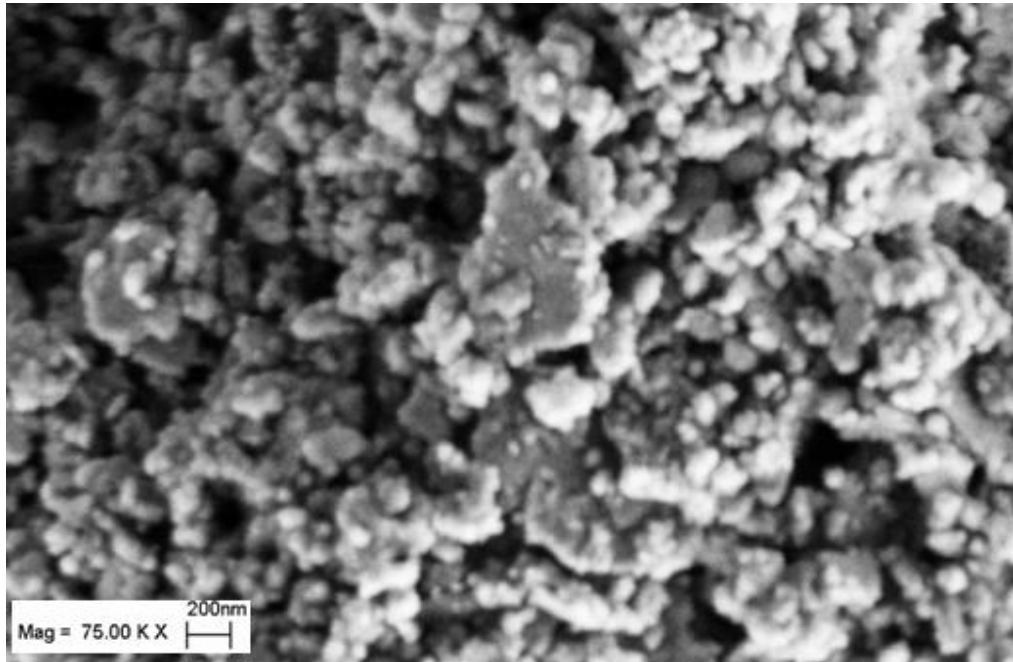


Figure 4.19: SEM Image of Ground Raw Perlite kept at 500°C for 10 minutes, 75000 Magnification

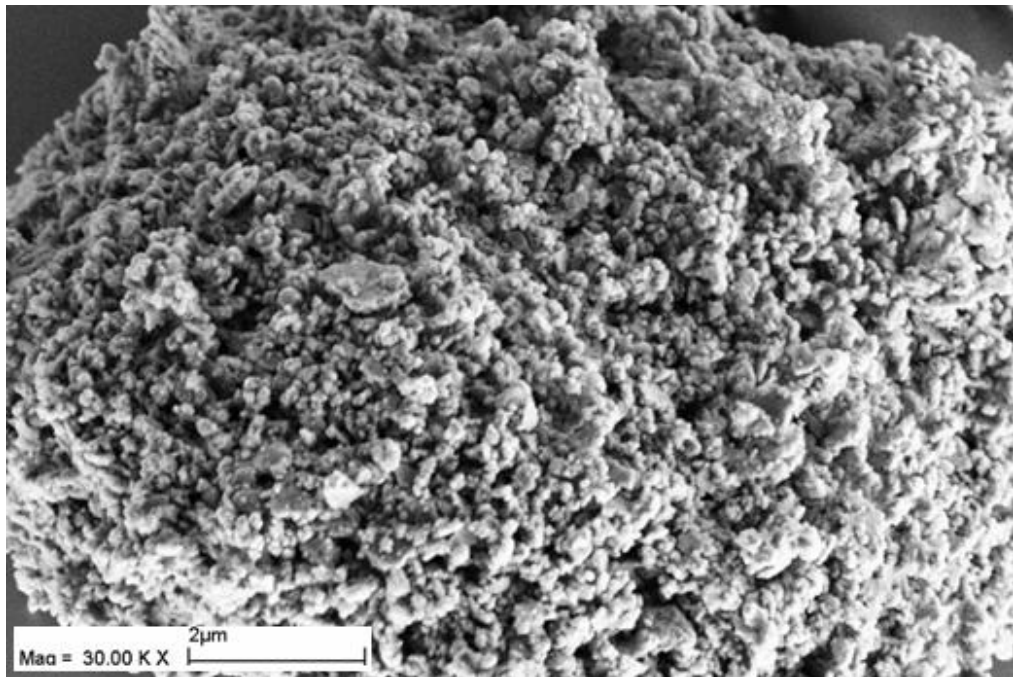


Figure 4.20: SEM Image of Ground Raw Perlite kept at 800°C for 10 minutes, 30000 Magnification

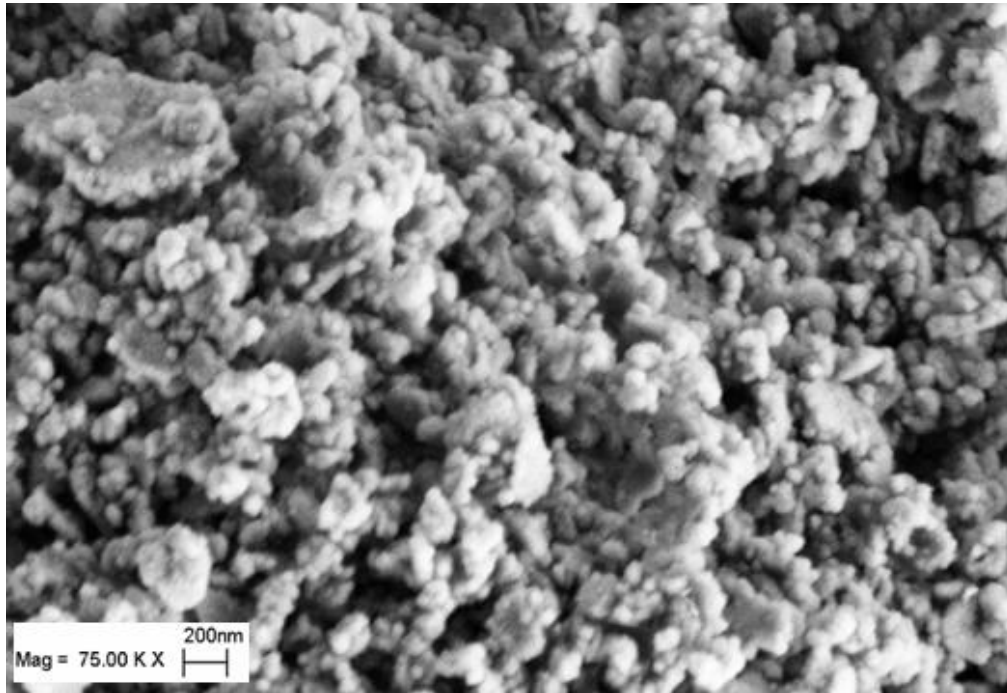


Figure 4.21: SEM Image of Ground Raw Perlite kept at 800°C for 10 minutes, 75000 Magnification

As it can be seen above, SEM images are paired; upper images show agglomerated particles which are between 8-10 microns whereas lower images show agglomerates which consist of small particles that are smaller than 100 nanometers in diameter. When magnification is increased, it is observed that perlite particles are becoming more oval. This could be due to a sintering effect or melting, or slightly related to the expansion of particles. However, there is no significant change in the size of observed particles. A potential change might be in the porosity of the perlite structure even though there is no decent expansion because of rapid heat treatment.

4.2.2.3. Pycnometer Analysis

After raw perlite is ground and heat treated, it is possible that if there is an expansion generated porous structure formation inside particles, it is possible that the density of heat treated raw perlite will be larger than its initial density; assuming that these pores are closed because they cannot be observed in electron microscopy. Therefore, it is expected that the density of unprocessed raw nano perlite will be bigger than that of heat processed perlite. In other words, if there was an expansion inside the perlite particles, their density would be expected to be lower. To this end, densities of perlite samples which have been expanded in section 4.2.2.5. were computed.

		Temperatures at Which Perlite is Heated					
Applied Temperature	Ground Raw Perlite	300°C	400°C	500°C	600°C	700°C	800°C
Density (g/cm³)	1.8853	1.7812	1.7359	1.5725	1.3178	1.2980	1.2914

Table 4.2: Pycnometer Analysis of Heat Treated Nano Raw Perlite Samples

There is a general trend of density reduction of the samples that were studied. The decrease in density might be an indication of porous structure formation inside perlite particles when raw perlite is attrition milled first and then expanded. There is a general trend for the sample densities which were treated between 300-800°C and this phenomenon could be due to the possibility that absorbed molecular water might not have escaped perlite when it was dried at 100°C inside a furnace, and when perlite sample was heated from 300°C until 800°C the probability that this molecular water evaporated could be the reason behind the decrease in density. Pycnometer analyses have been repeated and same results were obtained.

4.2.2.4. BET Surface Analysis

Using BET Surface Analyzer, the specific surface area of heat treated nano raw perlite samples were found to be 43.0, 42.9 and 42.7 m²/g (at 300°C, 500°C and 800°C, respectively). SEM results showed us that there is no visible expansion; however pycnometer results indicated that porous structure forms inside these particles which alter initial density of ground raw perlite, increasing pore size of particles. Therefore, the fact that there seems to be no increase in surface area in BET Surface results strengthens the argument that water inside perlite particles escape during drying. There is no further water release which prevents enlarging of particles and their surface area during expansion process.

4.2.2.5. Expansion Using Hot Stage Microscopy

Commercial perlite particle size ranges from a few hundred microns to millimeters. When raw perlite is expanded, it makes a highly porous structure with a large surface area. It is believed that if raw perlite is attrition milled and then expanded, it is possible to obtain particles with extremely small pores that are nanometers in size. To test this

hypothesis and the kinetics of the expansion, raw nano perlite was expanded using Hot Stage Microscope which would allow for a close investigation of perlite structure change as a function of temperature. Two different samples were used; one sample from Taşper Ltd., and the other one from Genper Ltd.

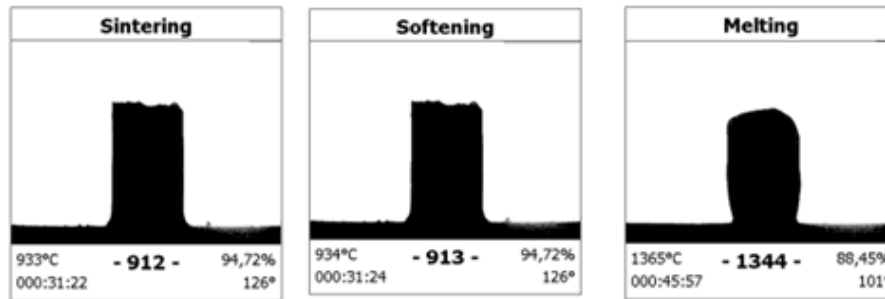


Figure 4.22: Expansion Character of Nano Raw Perlite (Taşper Ltd.)

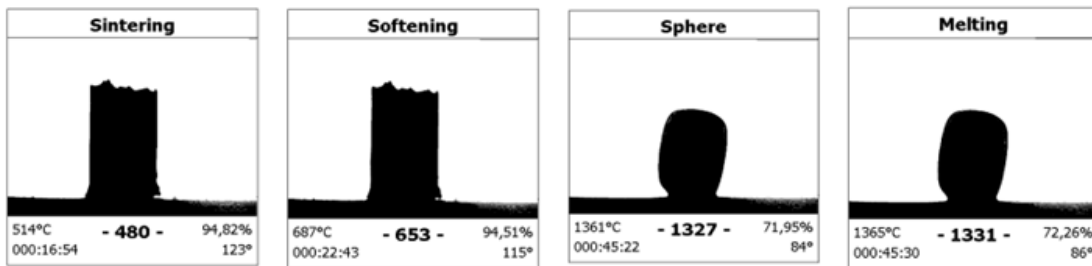


Figure 4.23: Expansion Character of Nano Raw Perlite (Genper Ltd.)

Perlite particles were applied heat inside the Hot Stage Microscope reservoir, with temperature increasing 30°C per minute. Perlite sample from Genper Ltd. starts sintering at 480°C, softens at 653°C, becomes a sphere at 1327°C and melts at 1331°C. The other perlite sample from Taşper Ltd. starts sintering at 912°C and softens at the same temperature, and melts at 1344°C. After this analysis, it is concluded that there is not expansion in perlite structure. However, it is understood that because the heating speed of the Hot Stage Microscope is slow, this type of process is not designed for perlite expansion. It is found out that only rapid heating can provide a drastic change in perlite structure causing it to expand 5-20 times its original volume.

4.3. Expanded Perlite Preparation and Characterization

4.3.1. Expanded Perlite Preparation

Ball Milling

Expanded perlite has been ball milled to incorporate it into PDMS; which in turn has resulted with an ability to feed concentrations of 20% without any trouble into attrition mill system. In ball milling method, ceramic balls rotate in horizontal axis for 24 hours inside a plastic drum along with expanded perlite. Using this method, expanded perlite which was millimeters in size has been reduced to a fine powder ready to be used.

Screening

Expanded perlite, which was ball milled first, was further processed to eliminate this contamination by being screened through 4 sifts which are 25 μm , 43 μm , 102 μm and 182 μm in mesh size. A vibrating motor was placed on bottom of sifts which were sitting on top of each other, with 182 μm on very top. Perlite was poured on top and 30 minutes of vibration was applied, this resulted in contamination being cleared from the fine powder.

4.3.2. Expanded Perlite Characterization

4.3.2.1. XRD Analysis

X-Ray Diffraction technique was employed to determine the crystal structure of expanded perlite. As it can be seen in below figure 4.1, there are no crystal peaks observed in the XRD spectra of expanded perlite in various particle size. This result confirms that the mineral has no crystal structure just like amorphous silica.

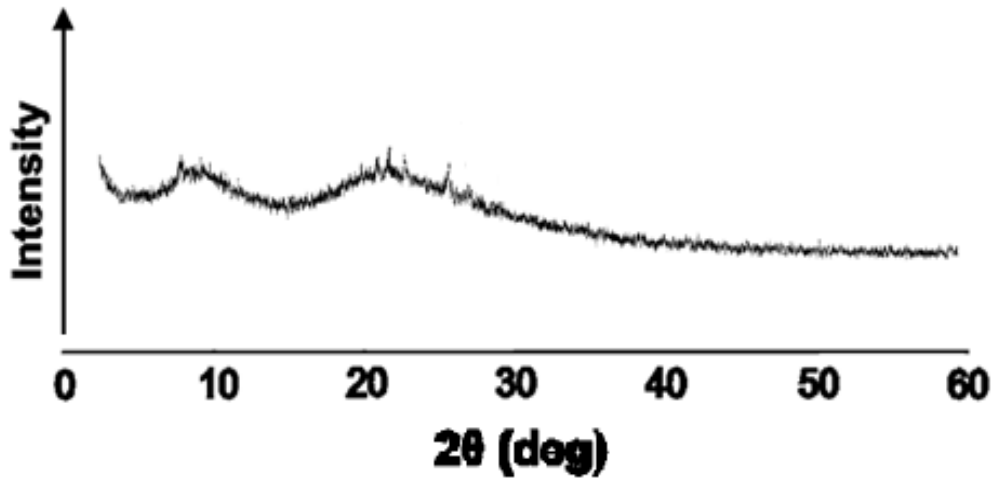


Figure 4.24: XRD Spectrum of Expanded Perlite

4.3.2.2. BET Surface Analysis

Using BET Surface Analyzer in laboratory premises, the specific surface area of expanded perlite was measured to be $7.5 \text{ m}^2/\text{g}$.

4.3.2.3. Pycnometer Analysis

At 20°C , density of expanded perlite was measured to be $1.2 \text{ gram}/\text{cm}^3$.

4.3.2.4. SEM Characterization

Scanning Electron Microscopy was used to analyze particle size and structure of expanded perlite was studied. As it can be seen in the below SEM images, expanded perlite has a platelet structure and its aspect ratio is much higher compared to amorphous silica. The wide size distribution of perlite particles can also be observed, which is also parallel to the Dynamic Light Scattering results.

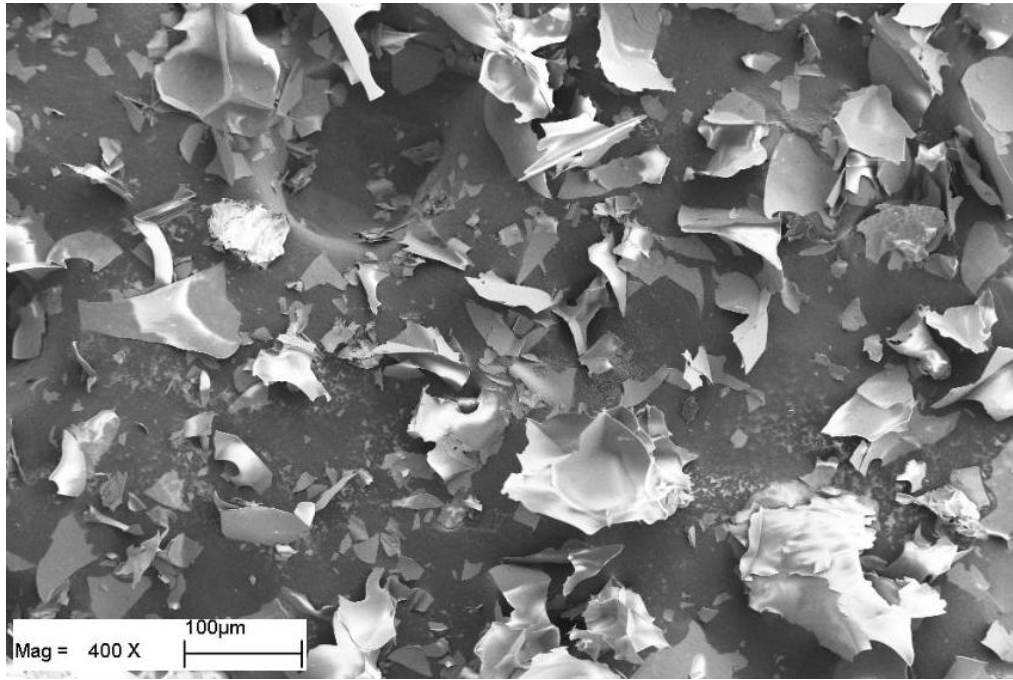


Figure 4.25: Expanded Perlite Particle at 4000 Magnification

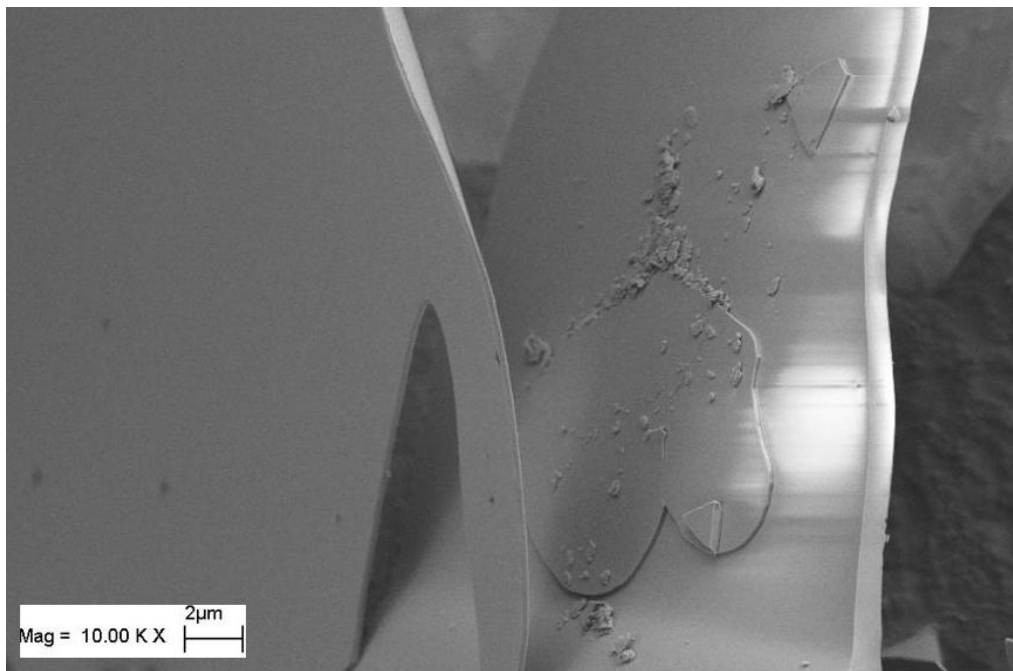


Figure 4.26: Expanded Perlite Particle at 10000 Magnification

4.3.2.5. Surface Titration

Titration has been carried to determine the hydroxyl (-OH) group density on expanded perlite surface. The result is calculated to be 0.0033 millimol/gram. Using the specific surface area ($48.88 \text{ m}^2/\text{g}$), the density of -OH groups on expanded perlite surface is $0.0406 \text{ -OH}/\text{nm}^2$. This result indicates that expanded perlite surface is ready to undergo modification to improve its compatibility with PDMS.

4.4. Nano Expanded Perlite Preparation, Characterization, and Elastomer Preparation

4.4.1. Nano Expanded Perlite Preparation and Characterization

4.4.1.1. Attrition Mill Process

The main goal in using the Attrition Mill is to reduce particle size expanded perlite to the nano scale. The Attrition Mill parameters were thoroughly considered and an optimization study was designed using the below parameters:

- Rotation speed was adjusted to 1800 rpm;
- Feeding rate was adjusted to 2; chosen as to keep perlite particles longer in the grinding environment;
- Bead size was 3mm;
- Suspension concentration was kept at 20 %;
- For the duration of run time of this optimization study, particles were ground as 90 minutes.

4.4.1.2. BET Surface Analysis

Using Intelligent Gravimetric Adsorption (IGA) shown in below figure in laboratory premises, the specific surface area of nano expanded perlite was calculated to be 48.2 m²/g.

4.4.1.3. Pycnometer Analysis

At 20°C, density of expanded perlite was calculated to be 1.2 gram/cm³.

4.4.1.4. Optimization Study & Dynamic Light Scattering

Same parameters and procedures in 4.2.1.2. were followed. Table 4.2 suggests that average particle size decreases up to 90 minutes of attrition milling. This result is parallel to results in studies done in 4.2.1.2. and same result was observed the same way when expanded perlite was attrition milled. Although average particle size slightly goes up when going from 90 to 120 minutes, it can be understood from figures 4.13 and 4.14 that average particle size is actually going down but the increase of agglomeration becomes more effective due to smaller particle size which can be seen in the curves that define the wide distribution.

DLS analysis shows that average particle size is 260 nm.

Milling Time (minutes)	Particle Size (nm)
5	440
15	364
30	309
45	275
60	274
90	260
120	263

Table 4.3: Attrition Mill optimization study recorded at constant feed rate and 1800 rpm. Right column shows Dynamic Light Scattering results. Unit is nanometers.

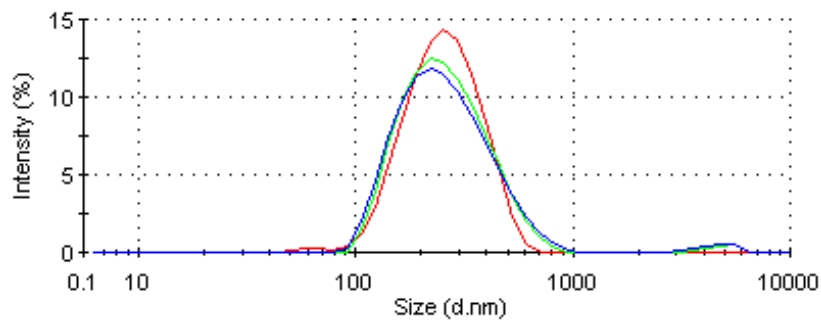


Figure 4.27: DLS Spectrum of Expanded Perlite after 60 minutes of Milling

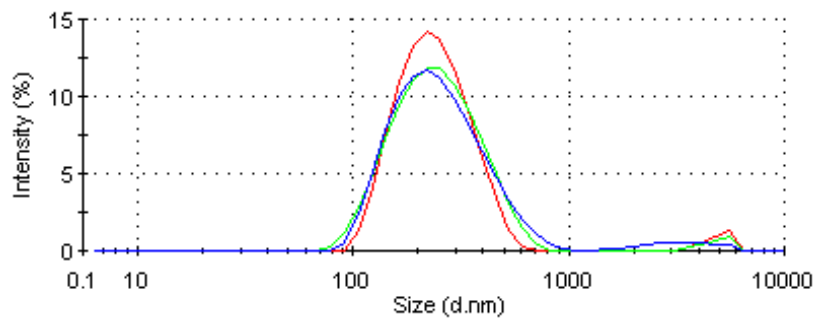


Figure 4.28: DLS Spectrum of Expanded Perlite after 90 minutes of Milling

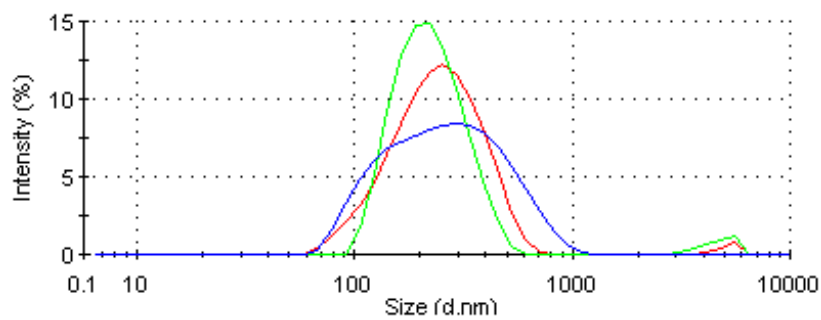


Figure 4.29: DLS Spectrum of Expanded Perlite after 90 minutes of Milling

4.4.1.5. SEM Characterization

SEM was used to analyze the particle shape of nano expanded perlite:

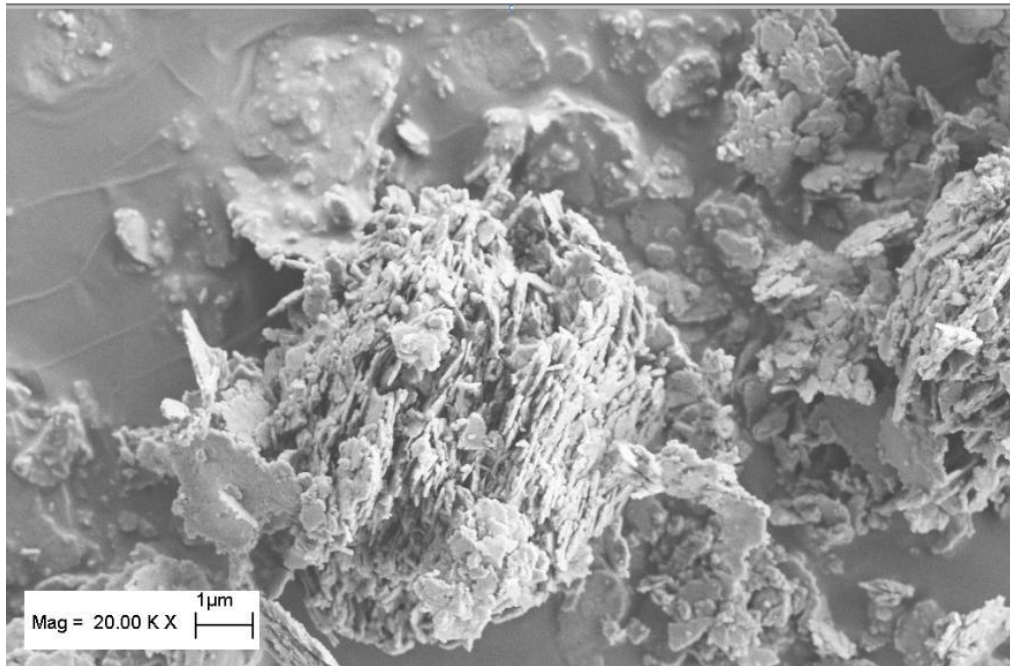


Figure 4.30: SEM Image of Ground Expanded Perlite at 20000 Magnification

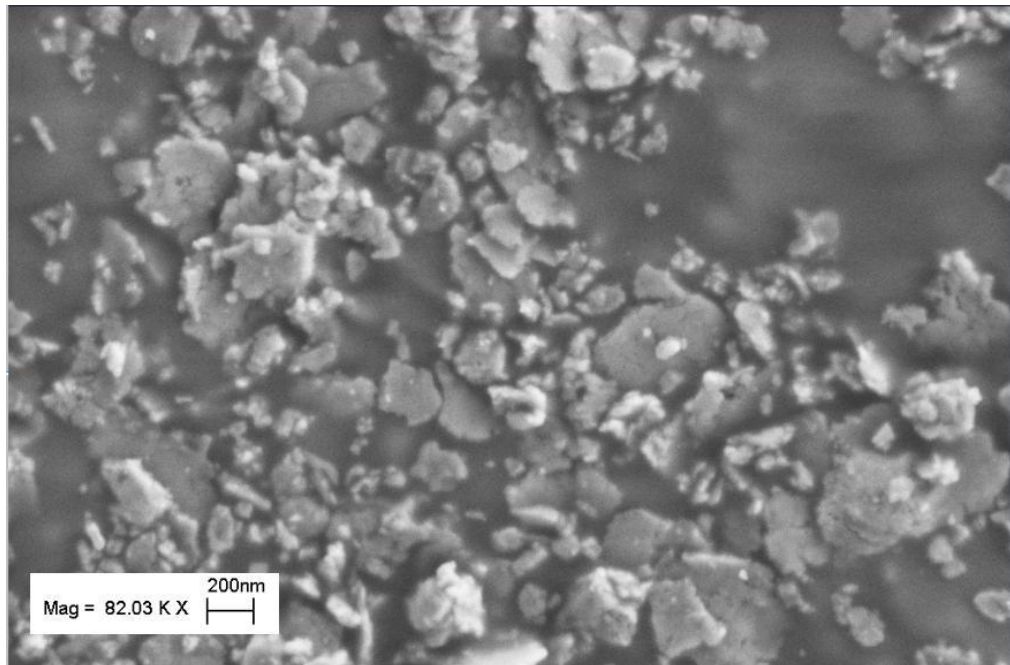


Figure 4.31: SEM Image of Ground Expanded Perlite at 82000 Magnification

It can be seen from figure 4.18 that as a result of attrition milling, one of the issues raised beyond the reduction of particle size, is the increase in agglomeration as it

becomes more effective. In figure 4.19, when particles making up agglomerates are closely investigated, it is seen that agglomerates in this image are made up of similar looking platelet shaped nano particles. It is important to note that average particle size is actually smaller than 100 nanometers (around 40-50 nm). One must remember that average particle size subjected to ultrasonic bath was around 400-500 nm. A potential conclusion is that agglomeration becomes increasingly more effective as particle size is decreasing, and that ultrasonic baths are not able to overcome and break agglomerates which results in DLS measurements in an higher average particle size than real size. After attrition milling, the fact that particle size distribution is more homogeneous than in a system not attrition milled, and that particle shape is getting increasingly more spherical are two reasons which might play roles in the observed agglomeration.

4.5. Surface Treated Nano Perlite Preparation, Characterization and Elastomer Preparation

4.5.1. Surface Treated Nano Perlite Preparation

In section 4.3.1.5., it was stated that there was adequate amount of –OH groups on perlite surface to undergo surface modification reactions. In this section, characterization analyses and results will be presented on the surface treated perlite using Hexamethyldisilazane. The reaction of Hexamethyldisilazane and silanol groups on perlite surface is as follows:



Using this reaction, it is thought that mineral surface is covered with an organosilane which enables the organic part to be more compatible with the polymer matrix. In order to prepare perlite-PDMS masterbatches using methods described in 3.5., the ratio of HMDS to nano expanded perlite that was used during mixing was taken from Gelest's Silane Coupling Agents: Connecting Across Boundaries manual. This way, surface modified hydrophobic nano-perlite has been prepared around 5 kilograms to be used in masterbatch preparation.

4.5.2. Surface Treated Nano Perlite Characterization

4.5.2.1. Fourier Transform Infrared Spectroscopy – FT-IR

Below figures show the FT-IR spectra of nano-perlite, before and after mixing it to treat its surface with Hexamethyldisilazane.

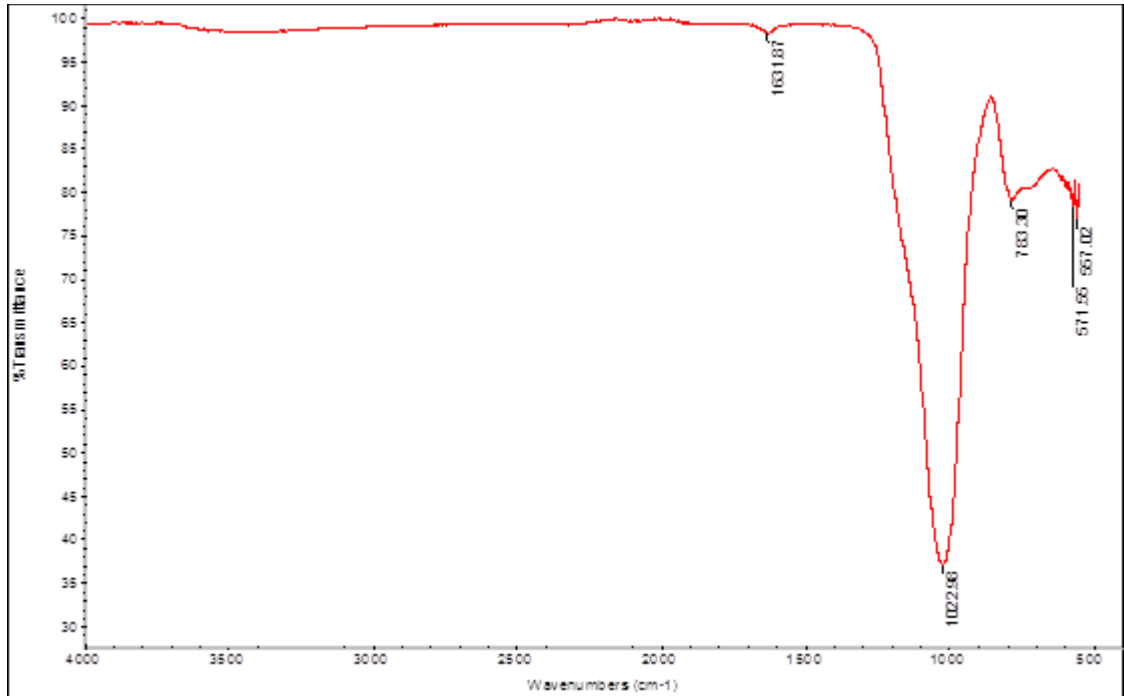


Figure 4.32: FT-IR Spectrum of Nano Expanded Perlite

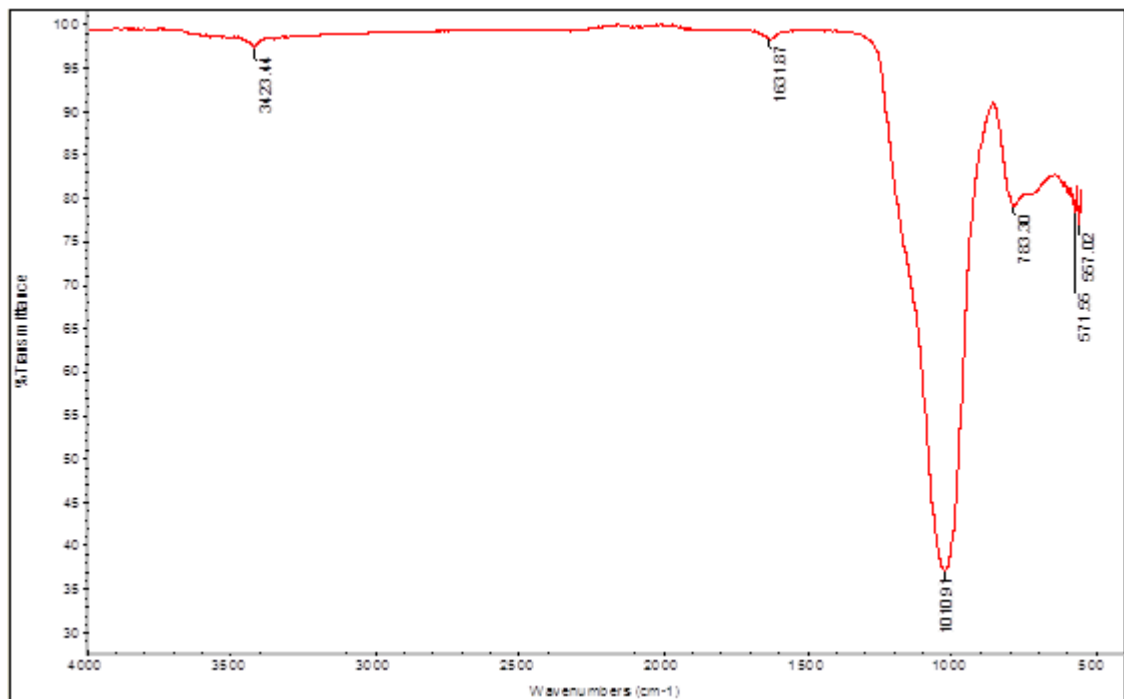


Figure 4.33: FT-IR Spectrum of Ground Nano Expanded Perlite after Hexamethyldisilazane Reaction and Being Dried at 100°C

In the first spectrum above, vibrational stretch peak belonging to the Si-OH functional group which is expected to be seen around 1000 cm^{-1} appears at 1022.98 cm^{-1} . Intensity of Si-OH groups' peaks in spectrum of perlite sample in the second figure appears weaker. When reacting with Hexamethyldisilazane, hydroxyl groups that exist on perlite surface create O-Si-O functional groups. Therefore, in figure 4.33, the decrease in the Si-OH vibrational stretch peaks' intensity might be due to the applied heat. As a result of treatment of Hexamethyldisilazane and being cured, it could be suggested that there is an increase in the number of hydrophobic perlite particles and a decrease in the number of hydrophilic particles on the surface of the mineral. However, the change in the signal belonging to Si-OH groups might be due to the amount of sample measured on the device and/or how much the tip of the FT-IR is penetrating the sample; therefore a comparison of proportions was deemed more suitable. So, the % transmittance value belonging to the peak seen around 1000 cm^{-1} was proportioned to the % transmittance value of the peak on the right side for each spectrum. Results show that this ratio was the highest for the first FT-IR spectrum of ground expanded nano-perlite, and lowered in the second spectrum. Hence, it can be concluded that these results show curing is responsible for the decreasing signal in vibrational stretch of Si-OH functional group.

4.5.2.2. Thermogravimetric Analysis

Below are the TGA analyses of the two perlite samples. As it can be seen on the first figure, the weight loss of ground expanded nano-perlite is around 2.6 %. On the second figure, TGA curve of perlite sample which has been treated with Hexamethyldisilazane and dried at 100°C is seen. According to the analyses, weight loss of sample is 4.3 %. In the second sample dried at 100°C , observed weight loss is almost 2 % more than the first unmodified sample. In the process of surface modification with Hexamethyldisilazane, alkoxy silane hydrolyzes, forms silane triols, condenses and creates oligomers and then siloxane polymers. $-\text{SiOH}$ groups make hydrogen bonds with the $-\text{OH}$ groups on the surface. As reaction proceeds, water comes out, covalent bond with the surface occurs and then the mineral surface is covered with an organosilane. Due to this reason, it can be concluded that the fact that there is more weight loss in an increasing order in samples is stemming from the formation of organic parts on perlite surface because of surface modification.

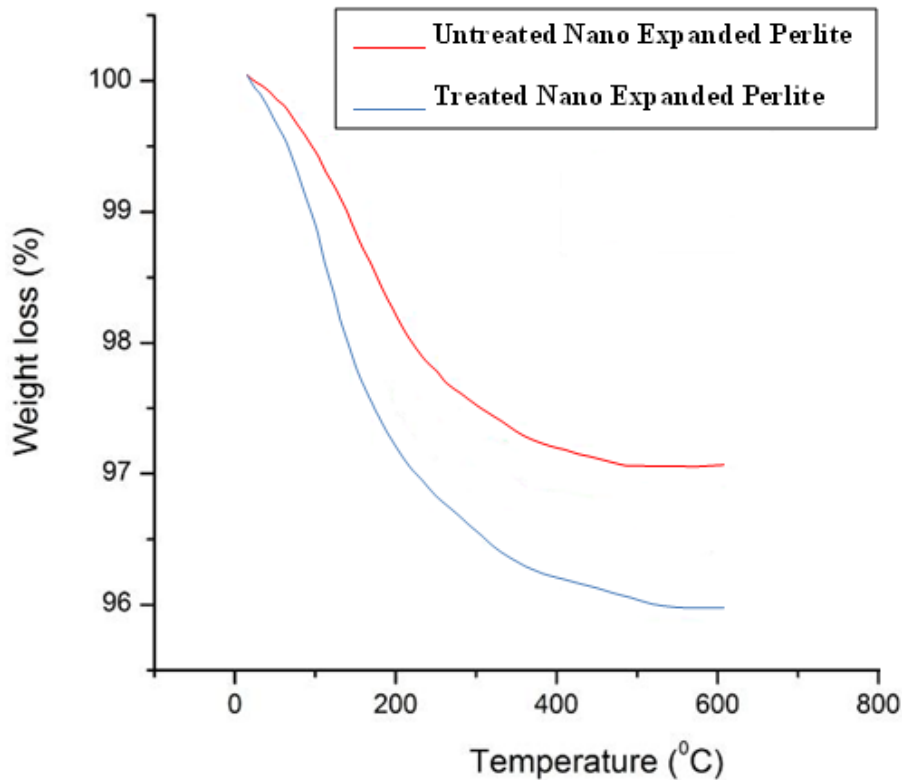


Figure 4.34: TGA Analyses of Nano Expanded Perlite and Nano Expanded Perlite after Hexamethyldisilazane Reaction and Being Dried at 100°C

4.6. Masterbatch and Elastomer Preparation

4.6.1. Using Nano Raw Perlite

4.6.1.1. Mixing PDMS and Perlite to Obtain Masterbatch

Commercial raw perlite was ball milled and screened to reduce its form to fine powder. Attrition milling was used to scale its particle size to nanometer. After obtaining nano raw perlite around 240 nm, perlite was ready to be mixed with PDMS in a closed system. As described in section 3.6. (Masterbatch Preparation), nano raw perlite was slowly added to the mixer tank, in which PDMS was already getting worked on by the butterfly arms to reduce its viscosity under high temperature.

4 different masterbatches were made ready to be tested for mechanical and rheological properties. First masterbatch was the Commercial Grade, and the remaining three masterbatches were nano raw perlite-PDMS composites with loading levels 10, 20 and 30 %, respectively. Masterbatches with loading levels higher than 30 % have not been prepared as more perlite cannot be incorporated into

PDMS during mixing. This stands out as a vital know-how in the composite making using perlite and silicone oil in this thesis.

4.6.1.2. Elastomer Formulation and Characterization

Mechanical Studies

Using the prepared masterbatches, elastomer formulations were generated. In order to obtain meaningful data, hydroxyl-terminated silicone oils (with the first one being low molecular weight and the second high molecular weight) were added to all the masterbatches in the same amount and under same conditions. Below are the four main elastomer formulations prepared:

I: 20 % Low Molecular Weight PDMS, 20 % High Molecular Weight PDMS, 60 % Target Masterbatch

II: 20 % Low Molecular Weight PDMS, 20 % High Molecular Weight PDMS, 60 % [10 % Nano Raw Perlite + 90 % Methyl-terminated PDMS]

III: 20 % Low Molecular Weight PDMS, 20 % High Molecular Weight PDMS, 60 % [20 % Nano Raw Perlite + 80 % Methyl-terminated PDMS]

IV: 20 % Low Molecular Weight PDMS, 20 % High Molecular Weight PDMS, 60 % [30 % Nano Raw Perlite + 70 % Methyl-terminated PDMS]

For mechanical tests (viscosity, hardness, tensile and tear strength), 5 samples in each category were used and mean of obtained values were reported:

Property	I	II	III	IV
Viscosity (cP)	12,000	10,650	13,731	17,025
Hardness (Shore A)	12	9	12	15
Tensile Strength (N/mm ²)	1.80	1.30	1.47	1.67
Elongation at break (%)	680	320	273	258
Tear Strength (N/mm)	5.8	3.2	3.9	4.6

Table 4.4: Mechanical Properties of Prepared Elastomers

It can be seen that tensile and tear strength of the elastomers prepared with nano raw perlite improve. We began to have hopes that perlite can be an alternative to silica as a reinforcing material because these results showed us that tensile and tear strength of

fourth formulation is almost equal to target formulation's values. Tear strength of samples increase with increasing loading levels of expanded perlite, which is also another encouraging result. Same can be said about viscosity and hardness values. It should be noted, however, that elongation at break values of formulations II, III and IV are not close to target formulation's value. It is most likely that this is due to poor interaction between silicone polymer and filler. Also, it can be argued that since nano raw perlite's BET surface area is less than that of nano expanded perlite, mechanical results of above samples are influenced negatively due to less stress transfer from matrix to mineral.

Rheological Studies

In order to determine and analyze the interactions between perlite particles and PDMS, and perlite particles between themselves it is essential to study the elastic and viscous moduli of the prepared masterbatches. Therefore, elastic and viscous moduli of the masterbatches which contain different filler loading levels are studied using the Rubber Process Analyzer 2000 under 1° strain angle and room temperature in the frequency sweep mode.

For rheology analyses, four different masterbatches were examined; first figure belongs to the target masterbatch, and the second one displays the rheological behavior of 10, 20 and 30 % filled masterbatches.

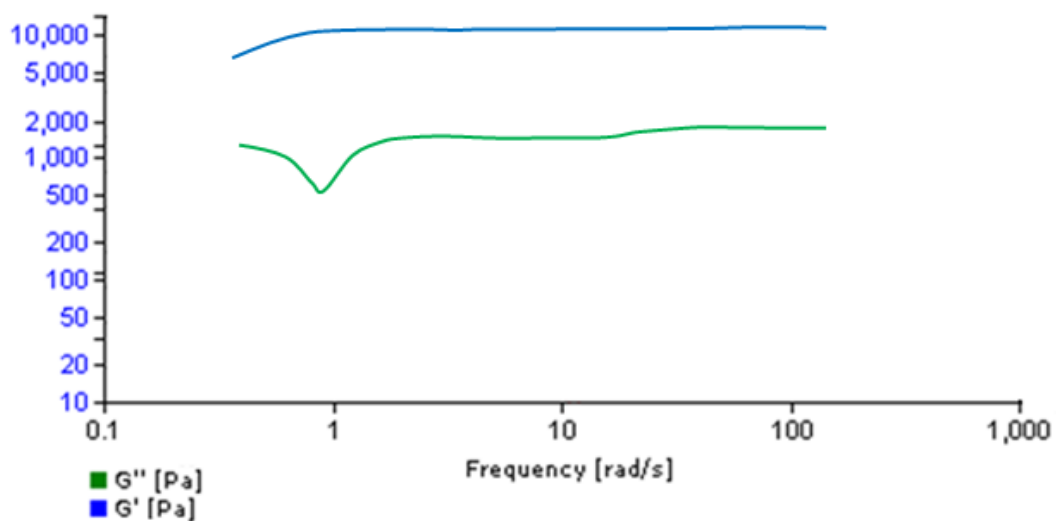


Figure 4.35: Target Masterbatch Frequency Sweep

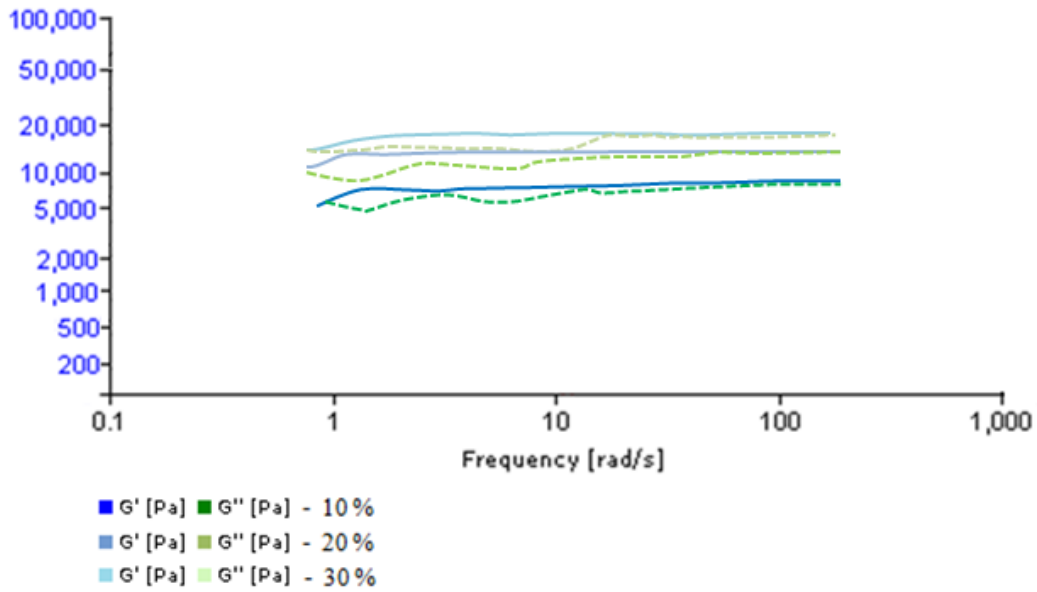


Figure 4.36: Frequency Sweep of 10, 20 and 30 % Filled Masterbatches (Nano Raw Perlite + Methyl-terminated PDMS)

Above masterbatches have been frequency swept and it is observed that the one that is closest to the target masterbatch in terms of elastic modulus (G') is the 20 % filled masterbatch; the elastic moduli of 10 and 30 % filled masterbatches are around 8000 Pa and 17000 Pa respectively, which are not close to that of the target masterbatch. 30 % filled masterbatch has much more network than the target masterbatch which might be due to filler loading level, or more silicone-perlite interactions in the system.

Viscous modulus will increase or decrease depending on the number of frictions between the aggregates which are formed by particles when agglomerates are distributed. All three of the prepared masterbatches have an higher viscous moduli (G'') when compared to the target masterbatch, this means that there is an high number of interaction between perlite particles.

All three of the prepared masterbatches have an higher viscous moduli (G'') when compared to the target masterbatch, this means that there is an higher number of interaction between perlite particles than there is between silica particles.

4.6.2. Using Expanded Perlite

4.6.2.1. Mixing PDMS and Perlite to Obtain Masterbatch

After ball milling and screening, expanded perlite was ready to be mixed with PDMS in a closed system. Similar to the schematics as described in section 3.6. (Masterbatch Preparation), expanded perlite was slowly added to the mixer tank, in which PDMS was already getting worked on by the butterfly arms to reduce its viscosity under high temperature.

4 different masterbatches were made ready to be tested for mechanical and rheological properties. First masterbatch was the Commercial Grade, and the remaining three masterbatches were expanded perlite-PDMS composites with loading levels 10, 20 and 30 %, respectively. Masterbatches with loading levels higher than 30 % have not been prepared as more perlite cannot be incorporated into PDMS during mixing.

4.6.2.2. Elastomer Formulation and Characterization

Mechanical Studies

Using the prepared masterbatches, elastomer formulations were produced. In order to generate meaningful data, hydroxyl-terminated silicone oils (with the first one being low molecular weight and the second high molecular weight) were added to all the masterbatches in the same amount and under same conditions. Below are the four main elastomer formulations prepared:

I: 20 % Low Molecular Weight PDMS, 20 % High Molecular Weight PDMS, 60 %
Target Masterbatch

II: 20 % Low Molecular Weight PDMS, 20 % High Molecular Weight PDMS, 60 %
[10 % Expanded Perlite + 90 % Methyl-terminated PDMS]

III: 20 % Low Molecular Weight PDMS, 20 % High Molecular Weight PDMS, 60 %
[20 % Expanded Perlite + 80 % Methyl-terminated PDMS]

IV: 20 % Low Molecular Weight PDMS, 20 % High Molecular Weight PDMS, 60 %
[30 % Expanded Perlite + 70 % Methyl-terminated PDMS]

For mechanical tests (viscosity, hardness, tensile and tear strength), 5 samples in each category were used and mean of obtained values were reported:

Property	I	II	III	IV
Viscosity (cP)	12,000	19,606	30,758	41,037
Hardness (Shore A)	12	19	23	28
Tensile Strength (N/mm ²)	1.80	1.67	1.96	2.12
Elongation at break (%)	680	255	205	170
Tear Strength (N/mm)	5.8	3.6	4.5	5.2

Table 4.5: Mechanical Properties of Prepared Elastomers

It can be seen that expanded perlite improves tensile and tear strength of the elastomers. The results are promising especially when tensile strength of third formulation is higher than first; this means that 20 % loading level, perlite can be an alternative to silica as a reinforcing material. Tear strength of samples increase with increasing loading levels of expanded perlite, which is also another good result. However, elongation at break values of formulations II, III and IV are not close to first formulation's value. This is possibly due to high particle size of expanded perlite particles. It is most likely that if particle size was reduced then more surface area would be created, which would account for more interaction between silicone polymer and filler. Viscosity and hardness values that were obtained are also way higher compared to target elastomer's values.

Rheological Studies

In order to determine and analyze the interactions between perlite particles and PDMS, and perlite particles between themselves it is essential to study the elastic and viscous moduli of the prepared masterbatches. Therefore, elastic and viscous moduli of the masterbatches which contain different filler loading levels are studied using the Rubber Process Analyzer 2000 under 1° strain angle and room temperature in the frequency sweep mode.

For rheology analyses, four different masterbatches were examined; first figure belongs to the target masterbatch, and the second one displays the rheological behavior of 10, 20 and 30 % filled masterbatches.

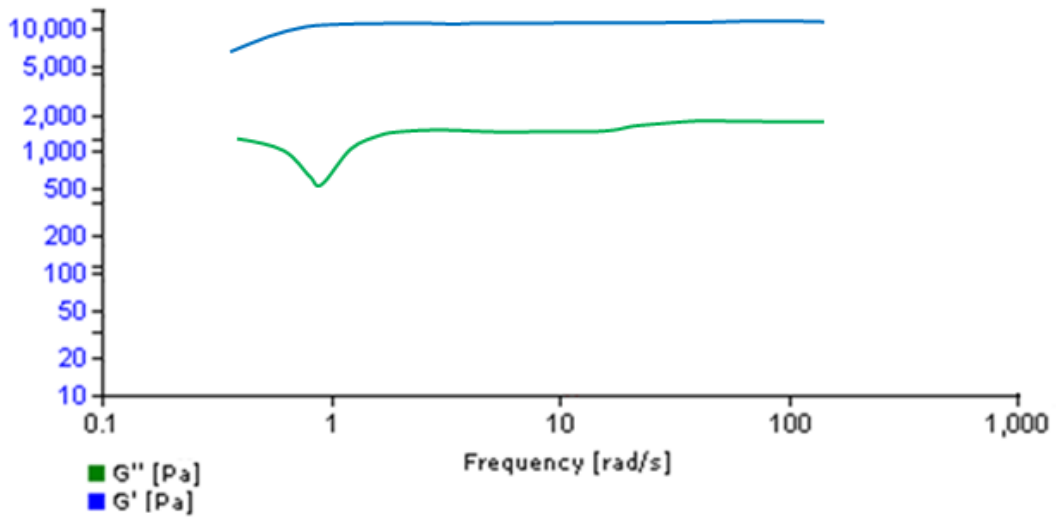


Figure 4.37: Target Masterbatch Frequency Sweep

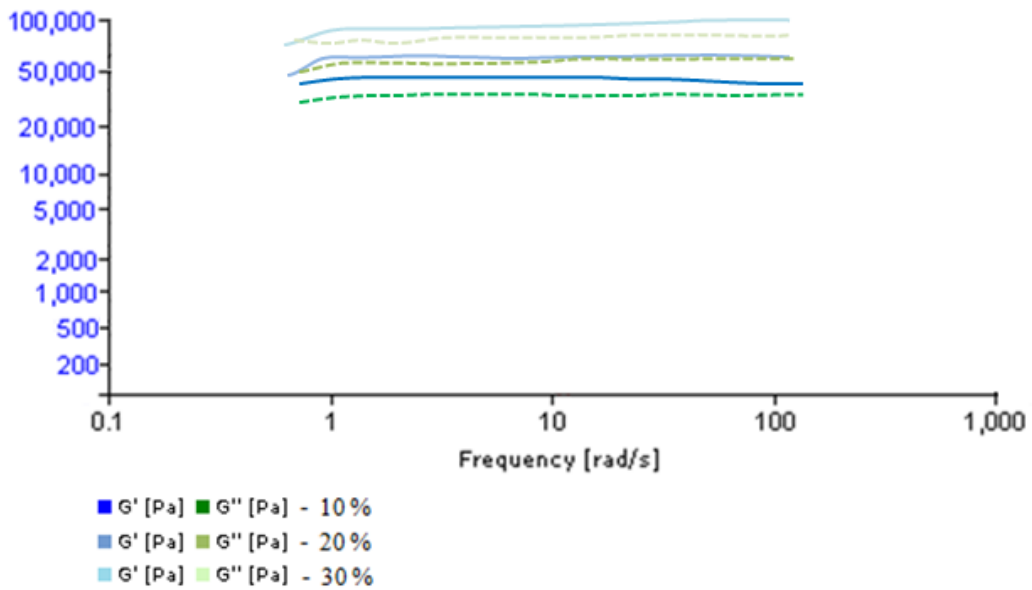


Figure 4.38: Frequency Sweep of 10, 20 and 30 % Filled Masterbatches (Expanded Perlite + Methyl-terminated PDMS)

From the masterbatches which have been frequency swept, one that is closest to the target masterbatch in terms of elastic modulus (G') is the 10 % filled masterbatch; the elastic moduli of 20 and 30 % filled masterbatches are around 60000 Pa and 80000 Pa respectively, which are very far away from that of the target masterbatch. It can be observed that the 10 % filled masterbatch has much more network than the target

masterbatch which might be due to filler loading level, or more silicone-perlite interactions in the system.

Viscous modulus will increase or decrease depending on the number of frictions between the aggregates which are formed by particles when agglomerates are distributed. All three of the prepared masterbatches have an higher viscous moduli (G'') when compared to the target masterbatch, this means that there is an high number of interaction between perlite particles.

As a general trend, it can be seen that expanded perlite provides only limited amount surface area to create interactions between the polymer and the filler due to having large radius. Therefore, masterbatches prepared with expanded perlite do not exhibit elastic and viscous moduli that are close to that of the target masterbatch.

4.6.3. Using Nano Expanded Perlite

4.6.3.1. Mixing PDMS and Perlite to Obtain Masterbatch

Similar to the schematics as described in section 3.6. (Masterbatch Preparation), nano expanded perlite was slowly added to the mixer tank, in which PDMS was already getting worked on by the butterfly arms to reduce its viscosity under high temperature. After ball milling and screening, nano expanded perlite was ready to be mixed with PDMS.

4 different masterbatches were made ready to be tested for mechanical and rheological properties. First masterbatch was the Commercial Grade, and the remaining three masterbatches were nano expanded perlite-PDMS composites with loading levels 10, 20 and 30 %, respectively. Masterbatches with loading levels higher than 30 % have not been prepared as more perlite cannot be incorporated into PDMS during mixing.

4.6.3.2. Elastomer Formulation and Characterization

Mechanical Studies

Using the prepared masterbatches, elastomer formulations were produced. In order to generate meaningful data, hydroxyl-terminated silicone oils (with the first one being low molecular weight and the second high molecular weight) were added to all the masterbatches in the same amount and under same conditions. Below are the four main elastomer formulations prepared:

I: 20 % Low Molecular Weight PDMS, 20 % High Molecular Weight PDMS, 60 % Target Masterbatch

II: 20 % Low Molecular Weight PDMS, 20 % High Molecular Weight PDMS, 60 % [10 % Nano Expanded Perlite + 90 % Methyl-terminated PDMS]

III: 20 % Low Molecular Weight PDMS, 20 % High Molecular Weight PDMS, 60 % [20 % Nano Expanded Perlite + 80 % Methyl-terminated PDMS]

IV: 20 % Low Molecular Weight PDMS, 20 % High Molecular Weight PDMS, 60 % [30 % Nano Expanded Perlite + 70 % Methyl-terminated PDMS]

For mechanical tests (viscosity, hardness, tensile and tear strength), 5 samples in each category were used and mean of obtained values were reported:

Property	I	II	III	IV
Viscosity (cP)	12,000	11,756	14,890	17,562
Hardness (Shore A)	12	10	12	15
Tensile Strength (N/mm ²)	1.80	1.42	1.67	1.83
Elongation at break (%)	680	360	315	282
Tear Strength (N/mm)	5.8	3.7	4.5	5.0

Table 4.6: Mechanical Properties of Prepared Elastomers

Nano expanded perlite improves tensile and tear strength of the elastomers. The results are hopeful especially when tensile of strength of fourth formulation is higher than first; this means that at higher loading levels, perlite can be an alternative to silica as a reinforcing material. Tear strength of samples increase with increasing loading levels of expanded perlite, which is also another encouraging result. However, elongation at break values of formulations II, III and IV are not close to first formulation's value. This is possibly due to the fact that perlite particles need to be more compatible with silicone, and conceivably go under surface modification to make it hydrophobic. Also, it should be noted that competitive overall mechanical results shows that more surface area was created when particle size was reduced, which then accounted for more interaction between silicone polymer and filler.

Rheological Studies

Elastic and viscous moduli of the prepared masterbatches were studied in order to determine and analyze the interactions between perlite particles and PDMS, and perlite particles between themselves. Different filler loading levels were tested using the Rubber Process Analyzer 2000 under 1° strain angle and room temperature in the frequency sweep mode.

For rheology analyses, four different masterbatches were examined; first figure belongs to the target masterbatch, and the second one displays the rheological behavior of 10, 20 and 30 % filled masterbatches.

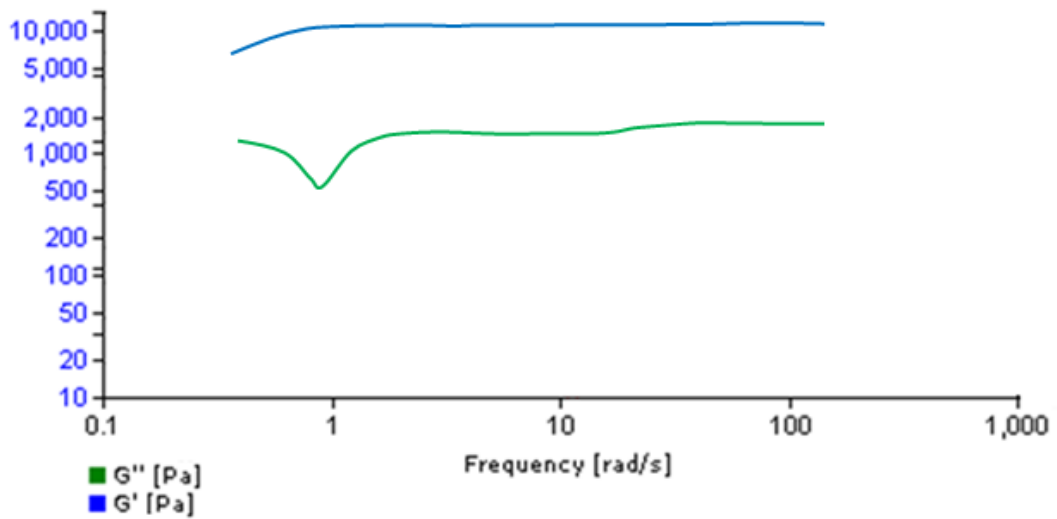


Figure 4.39 Target Masterbatch Frequency Sweep

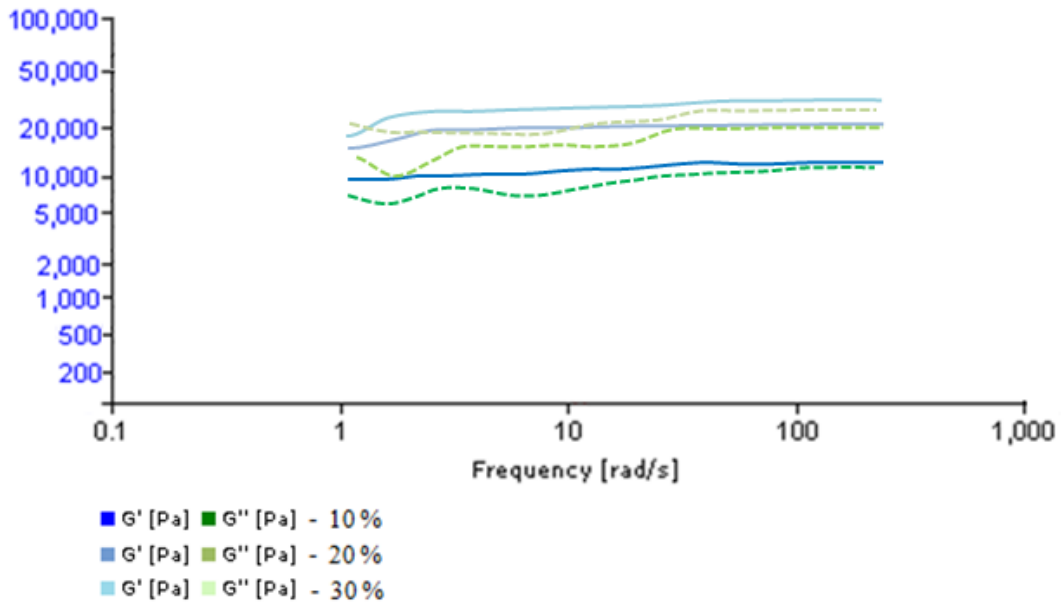


Figure 4.40: Frequency Sweep of 10, 20 and 30 % Filled Masterbatches (Nano Expanded Perlite + Methyl-terminated PDMS)

As a general trend, it can be seen that nano expanded perlite accounts for more surface area to create interactions between the polymer and the filler due to having small radius. Therefore, masterbatches prepared with nano expanded perlite exhibit elastic and viscous moduli that are relatively close to that of the target masterbatch.

From the masterbatches which have been frequency swept, one that is closest to the target masterbatch in terms of elastic modulus is the 10 % filled masterbatch (12000 Pa) again, similar to what has been observed in formulations prepared with expanded perlite. Elastic moduli of 20 and 30 % filled masterbatches are around 18000 Pa and 29000 Pa respectively, which are not very close to that of the target masterbatch. It can be seen that the 10 % filled masterbatch has same amount of network as the target masterbatch.

All three of the prepared masterbatches have an higher viscous moduli (G'') when compared to the target masterbatch, this means that there is still an higher number of interaction between nano expanded perlite particles.

4.6.4. Using Surface Modified Nano Expanded Perlite

4.6.4.1. Mixing PDMS and Perlite to Obtain Masterbatch

Similar to the schematics as described in section 3.6. (Masterbatch Preparation), nano expanded perlite was slowly added to the mixer tank, in which PDMS was already getting worked on by the butterfly arms to reduce its viscosity under high

temperature. After ball milling and screening, nano expanded perlite was ready to be mixed with PDMS.

4 different masterbatches were made ready to be tested for mechanical and rheological properties. First masterbatch was the Commercial Grade, and the remaining three masterbatches were surface modified nano expanded perlite-PDMS composites with loading levels 10, 20 and 30 %, respectively. Masterbatches with loading levels higher than 30 % have not been prepared as more perlite cannot be incorporated into PDMS during mixing.

4.6.4.2. Elastomer Formulation and Characterization

Mechanical Properties

For mechanical studies, four different masterbatches were used. First masterbatch is the target masterbatch, second masterbatch is 10 % nano-perlite filled, third masterbatch is 20 % nano-perlite filled, and fourth masterbatch is 30 % nano-perlite filled. The other component of the masterbatches is the low molecular weight methyl-terminated PDMS. From the four masterbatches, elastomer formulations are prepared where a formulation contains 20 % OH-Terminated low molecular weight PDMS by weight, 20 % OH-Terminated high molecular weight PDMS by Weight and 60 % masterbatch itself. Preparing an additional elastomer formulation using the target masterbatch, there are 4 different elastomers below that were mechanically tested using an Instron Universal Testing Machine.

Property	I	II	III	IV
Viscosity (cP)	12,000	7,896	10,625	13,357
Hardness (Shore A)	12	7	9	14
Tensile Strength (N/mm ²)	1.80	1.51	1.65	1.78
Elongation at break (%)	680	650	585	548
Tear Strength (N/mm)	5.8	4.6	5.1	5.6

Table 4.7: Mechanical Results of Prepared Elastomers

I: % 20 OH-Term. Low Molecular Weight PDMS, % 20 OH-Term. High Molecular Weight PDMS, % 60 Target Masterbatch

II: % 20 OH-Term. Low Molecular Weight PDMS, % 20 OH-Term. High Molecular Weight PDMS, % 60 Masterbatch 1

III: % 20 OH-Term. Low Molecular Weight PDMS, % 20 OH-Term. High Molecular Weight PDMS, % 60 Masterbatch 2

IV: % 20 OH-Term. Low Molecular Weight PDMS, % 20 OH-Term. High Molecular Weight PDMS, % 60 Masterbatch 3

It appears that mechanical properties of cured elastomers using the masterbatches prepared are competitive when compared with the mechanical properties of the first formulation, prepared using the target masterbatch. The results are very promising especially when tensile, tear strength values and elongation at break percentages are pretty close to each other. It can be seen that with the increasing level of filler loading, elongation at break continues to go down, but in this case difference is much less significant.

The fact that mechanical properties of the surface treated nano-perlite filled elastomers are close to the mechanical properties of target elastomer could be due to a few reasons: Expanded perlite is first nano-scaled to attain smaller particles and its surface is improved by a treatment process; this creates many enhanced interactions and compatibility between the filler and the polymer. Secondly, perlite possesses a flake/platelet shape and therefore an higher aspect ratio compared to the amorphous silica. Because of this platelet structure, stress transferred from the polymer matrix is able to be transmitted to a larger surface area when compared to silica and hence stress applied to the polymer was able to be distributed more homogeneously. Thirdly, due to the surface modification using Hexamethyldisilazane, perlite has been wetted by the polymer matrix much easier, agglomeration was avoided and perlite has mixed more homogeneously with the matrix.

Rheology of Prepared Masterbatches

Elastic and viscous moduli of the masterbatches which contain different filler loading levels were studied using the Rubber Process Analyzer 2000 under 1° strain angle and room temperature in the frequency sweep mode.

For rheology analyses, four different masterbatches are examined; first masterbatch is the target, second masterbatch contains 10 % surface modified nano-perlite by weight, third masterbatch contains 20 % surface modified nano-perlite by weight, fourth masterbatch contains 30 % surface modified nano-perlite by weight.

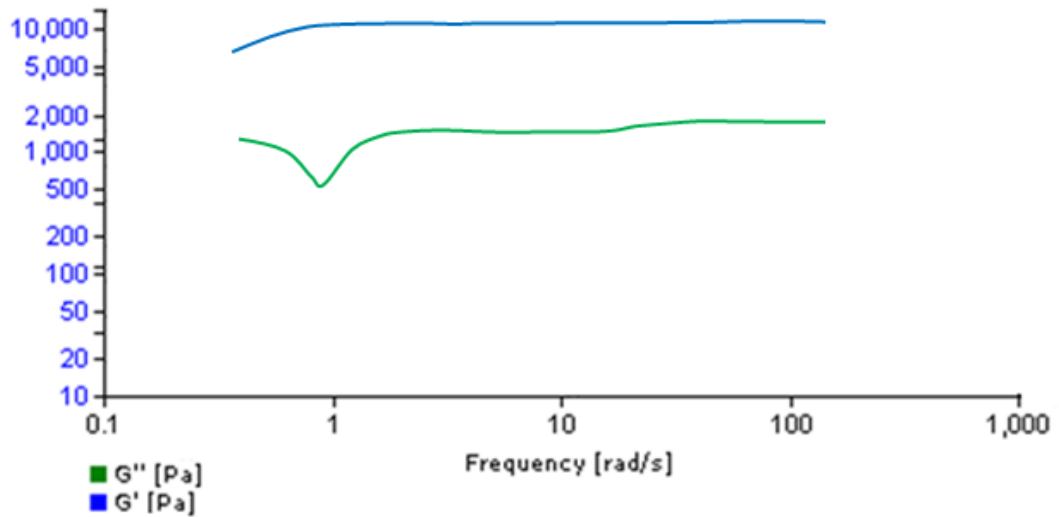


Figure 4.41: Target Masterbatch Frequency Sweep

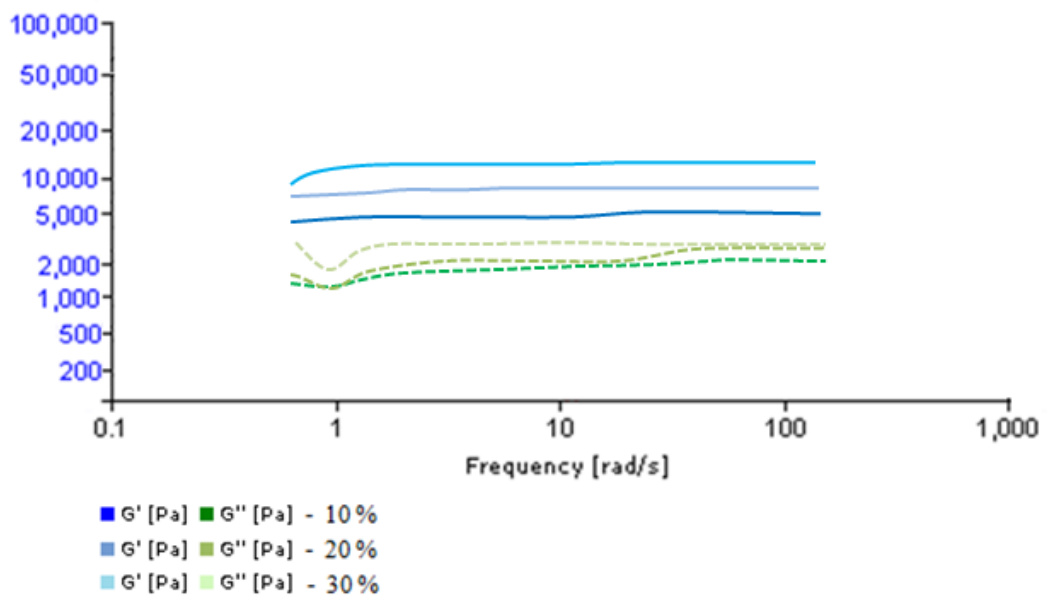


Figure 4.42: Frequency Sweep of 10, 20 and 30 % Filled Masterbatches (Surface Treated Nano Expanded Perlite + Methyl-terminated PDMS)

From the masterbatches which have been frequency swept, one that is closest to the target masterbatch in terms of elastic modulus (G') is the third masterbatch; the elastic moduli of second and third masterbatches are around 5000 Pa and 8000 Pa, which are also not very far away from that the target masterbatch. It can be observed that the third masterbatch has as much network as the target masterbatch due to an higher filler loading level, which accounts for more silicone-perlite interactions in the system.

All three of the prepared masterbatches have a similar viscous moduli (G'') when compared to that of target masterbatch, this means that there is a good number of interaction between perlite particles. It is observed that viscous moduli of samples are close to each other and the target masterbatch, which is directly linked to the compatibility of perlite with PDMS. Due to higher compatibility, there is greater matrix wetting and adhesion. Surface treated nano perlite provides more surface area to create more interactions between the polymer and the filler due to having small radius, which makes for more stable rheological structures.

Analyzing Particle Distribution in the System

To study nano-perlite particle distribution in the cured elastomer formulations, a cross sectional area from a mechanically tested sample is taken from elastomer formulation IV since it exhibits the best mechanical properties.

In figure 4.43, SEM image of 30 % filled elastomer formulation is given at 8000 magnification. It is safe to say that particle distribution is good and particles are generally homogeneously distributed. In figure 4.45, it can be seen that average particle size is around 200 nm, but due to agglomeration there are agglomerates which are 1-2 μm in size.

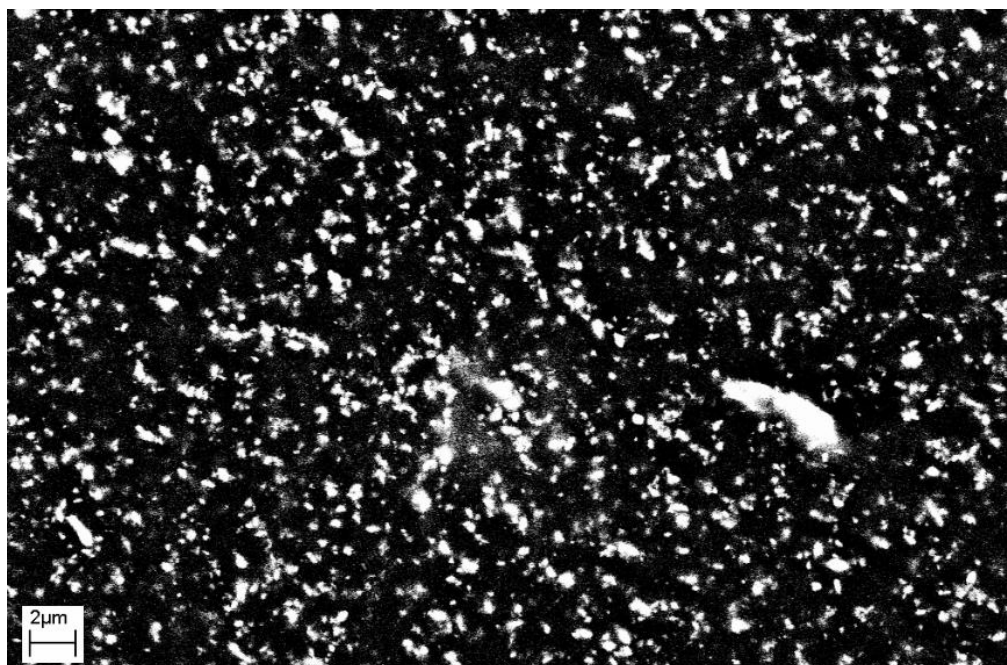


Figure 4.43: SEM Image of Elastomer Formulation IV at 8000 Magnification Using Backscattered Electron Detector

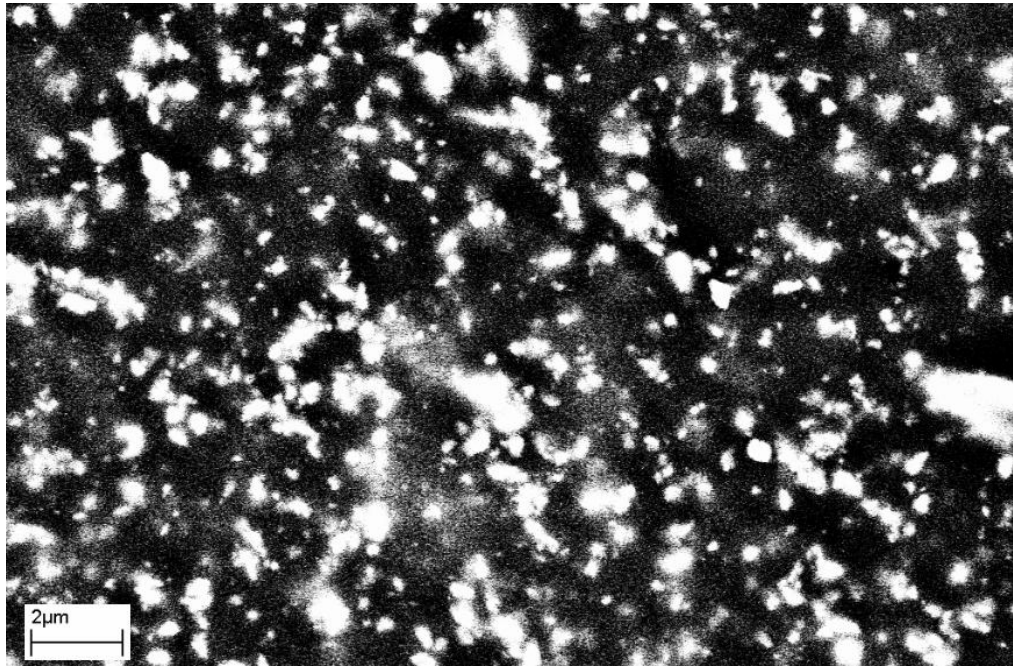


Figure 4.44: SEM Image of Elastomer Formulation IV at 16000 Magnification Using Backscattered Electron Detector

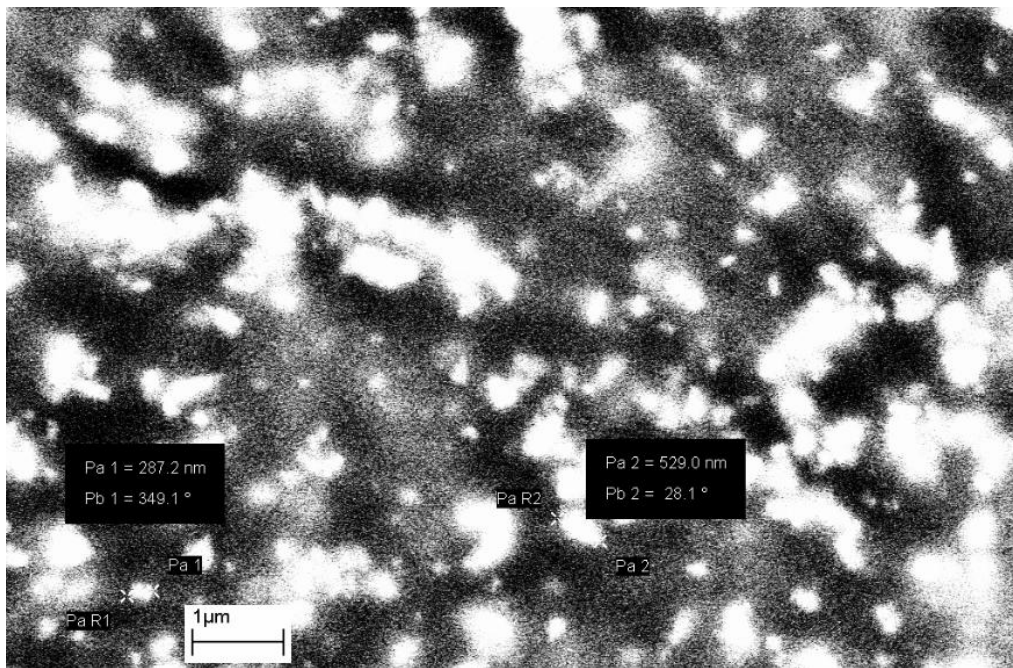


Figure 4.45: SEM Image of Elastomer Formulation IV at 32000 Magnification Using Backscattered Electron Detector

When figure 4.46 is examined, it is seen that nano-scaled perlite forms agglomerations which are 30-40 microns in diameter. This type of agglomeration might naturally have negative effects on the mechanical properties of the elastomer, which were observed in

mechanical results earlier; formulation IV has slightly reduced tensile and tear strength values, and a reduced elongation at break value.

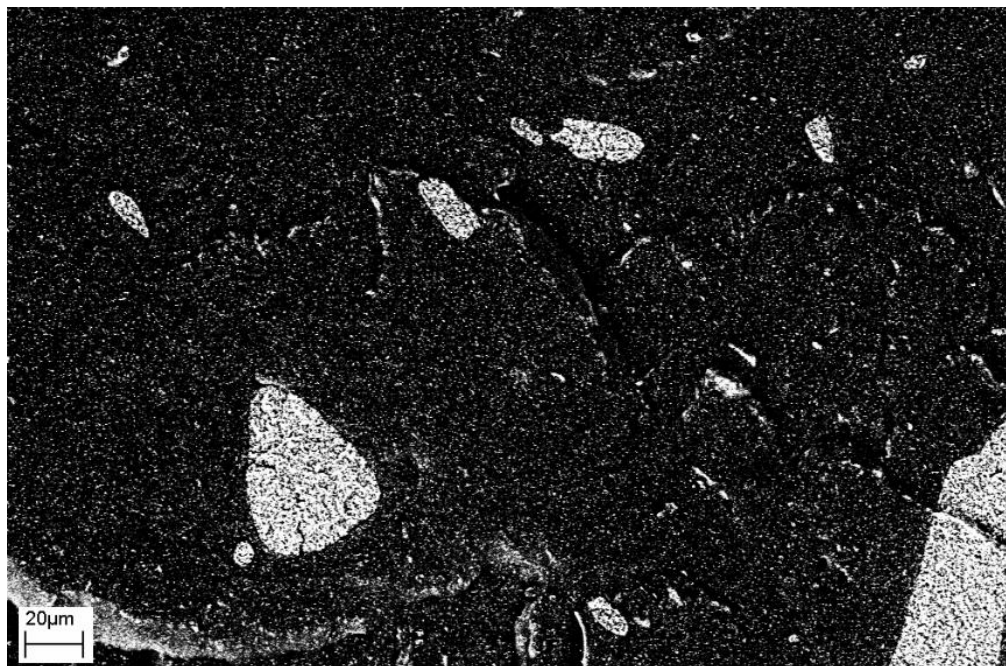


Figure 4.46: SEM Image of Elastomer Formulation IV at 1000 Magnification Using Backscattered Electron Detector

In figures 4.47 and 4.48 of 2000 and 16000 magnification, it is seen that silica particles in the target elastomers are well distributed. It is assumed that these hydrophobic silica particles are also surface treated due to less agglomeration observed in these images and an efficient homogeneous distribution in the polymer matrix which can be seen in the mechanical results.

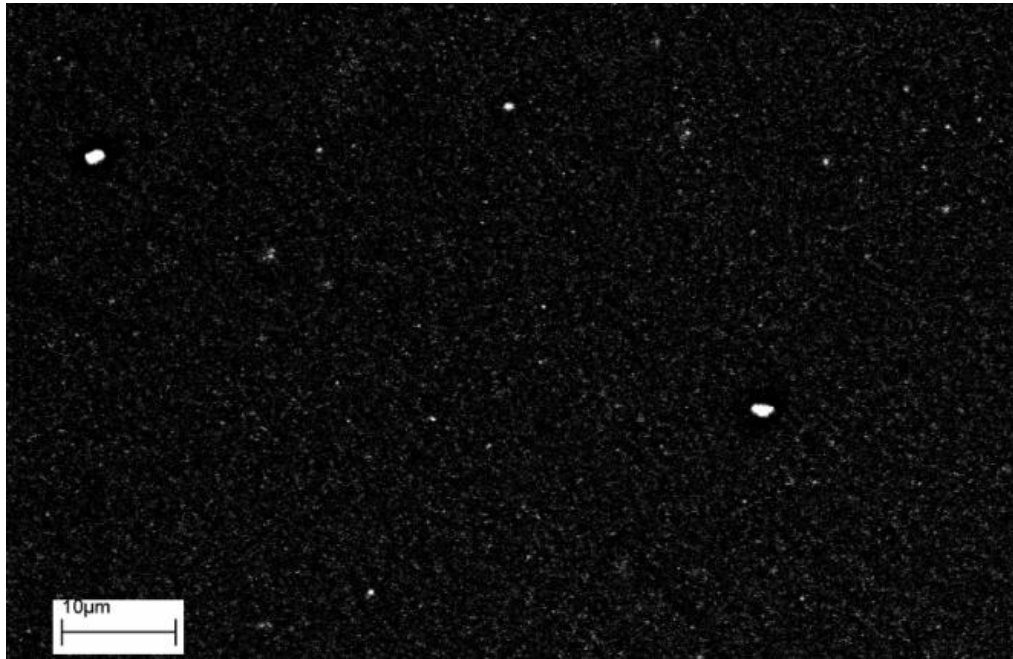


Figure 4.47: SEM Image of Target Elastomer at 2000 Magnification Using Backscattered Electron Detector

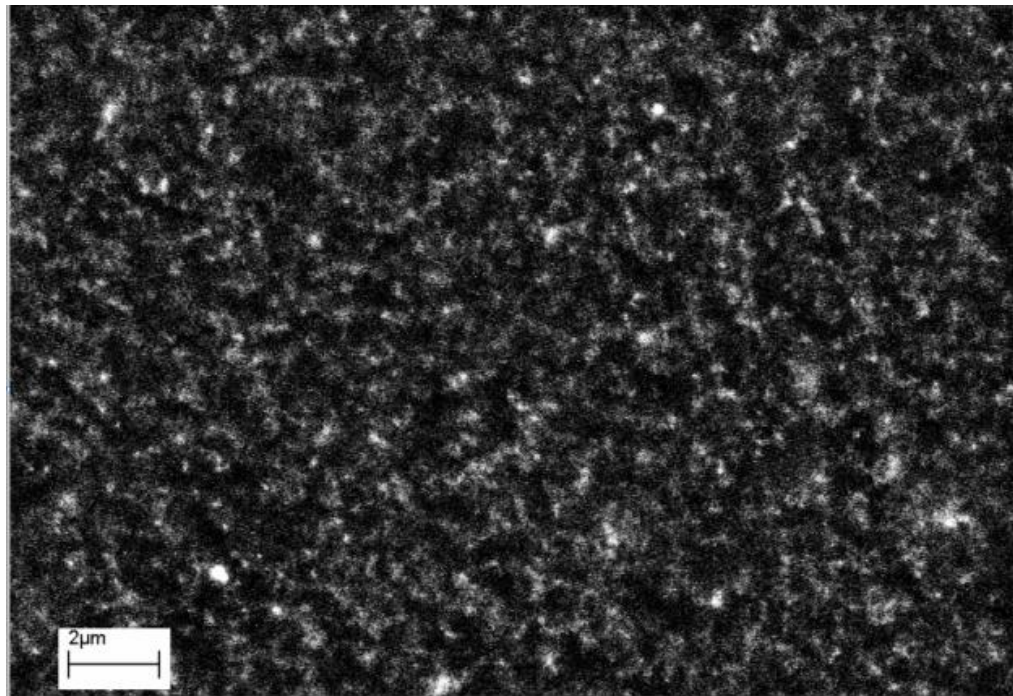


Figure 4.48: SEM Image of Target Elastomer at 16000 Magnification

4.7. Summary of Mechanical Results of Prepared Elastomers

To enhance understanding and make life easier, mechanical properties (Viscosity, hardness, tensile strength, elongation at break and tear strength) of elastomers have been placed in below charts:

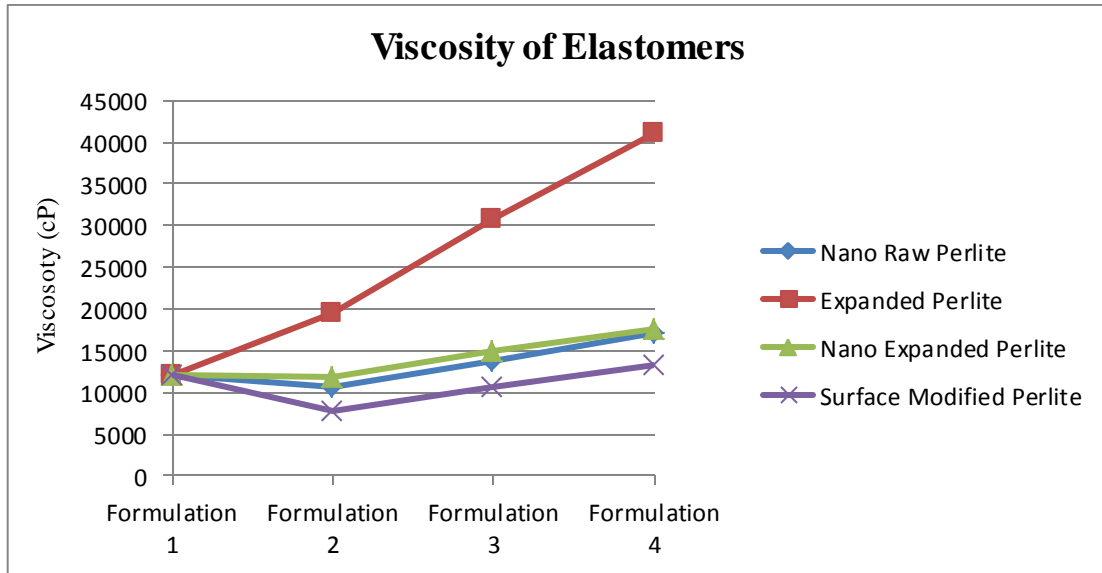


Figure 4.49: Viscosity of Prepared Elastomers Using 4 Different Types of Perlite

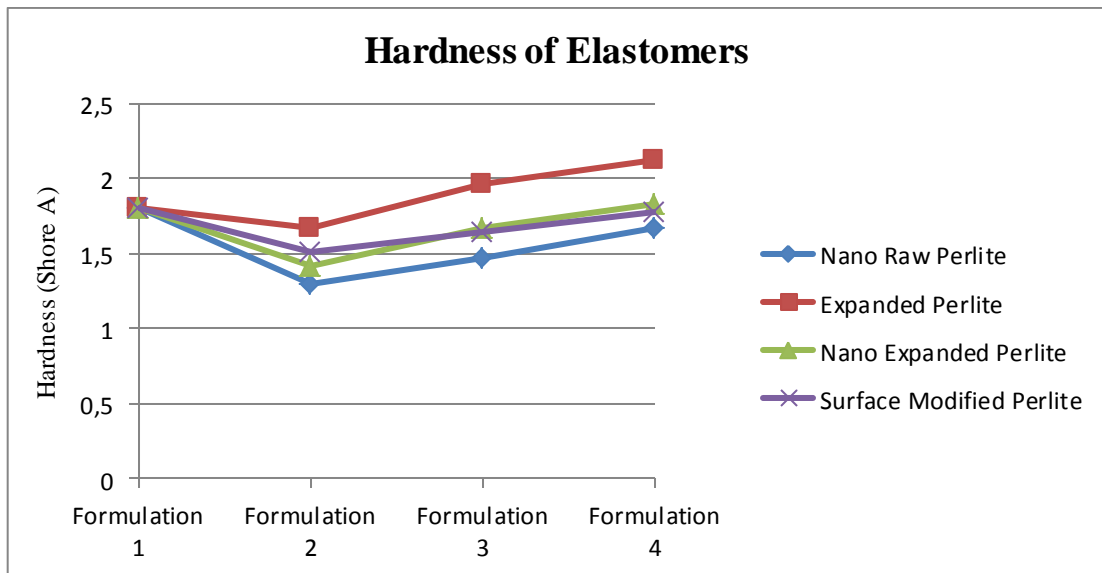


Figure 4.50: Hardness of Prepared Elastomers Using 4 Different Types of Perlite

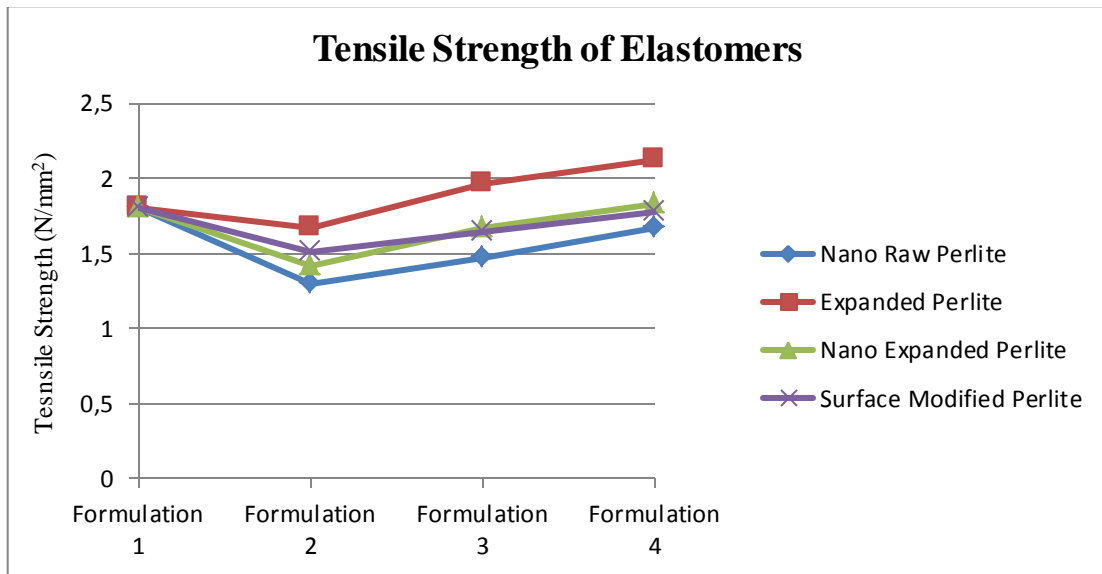


Figure 4.51: Tensile Strength of Prepared Elastomers Using 4 Different Types of Perlite

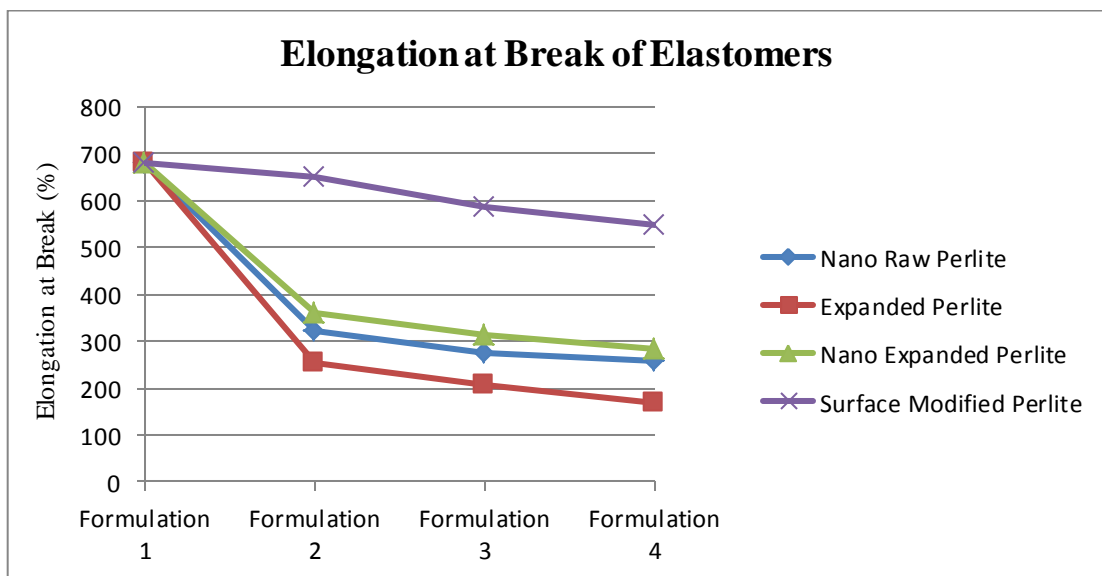


Figure 4.52: Elongation at Break of Prepared Elastomers Using 4 Different Types of Perlite

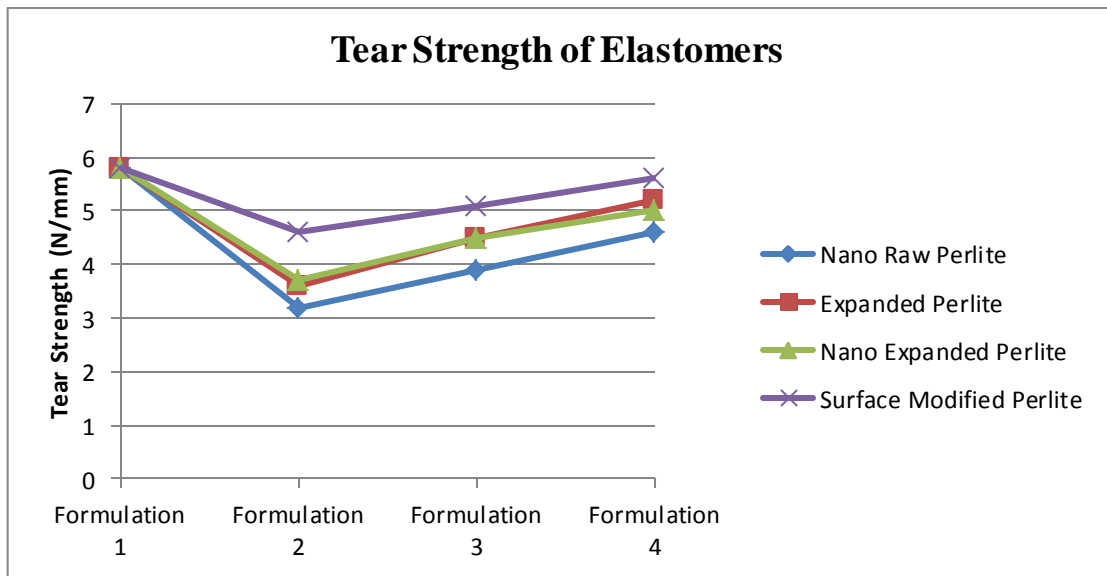


Figure 4.53: Tear Strength of Prepared Elastomers Using 4 Different Types of Perlite

CHAPTER 5

5. Conclusions

5.1 Conclusion

In this study, expanded and raw perlite as well as nano expanded and raw perlite were all tested as alternative fillers to silica in PDMS composites. To this end, perlite was first ball milled and screened to get rid of impurities. Second, filtered perlite in a fine powder form was ground using an Attrition Mill. Nano-perlite was further characterized by XRD analysis, surface titration, pycnometer analysis, BET surface analysis, Dynamic Light Scattering and Scanning Electron Microscopy. Raw perlite was also attrition milled, and its expansion character was studied using Hot Stage Microscopy, pycnometer analysis, Scanning Electron Microscopy and Dynamic Light Scattering. Nano-perlite was surface modified; surface improved nano-perlite was characterized using Fourier Transform Infrared Spectroscopy and Thermogravimetric analysis. PDMS – Nano-Perlite masterbatches were prepared; cured elastomer formulations were prepared and characterized by Universal Testing Machine, Rubber Process Analyzer and Scanning Electron Microscopy. As a result of these studies, the following observations were concluded;

- Ball milling and sifting commercial perlite was able to clear all contamination from the mineral. XRD analysis showed that perlite does not have a crystal structure. BET surface analysis indicated perlite's surface area is 48.88 m²/g; surface titration results showed that the –OH group density was 0.0033 millimol/g; two results combined that the number hydroxyl groups on perlite surface was 0.0406 –OH/nm², which is enough for surface modification.
- SEM showed that perlite has a platelet structure and its aspect ratio is higher than that of silica. The wide size distribution of particles was also observed. At room temperature, the density of expanded perlite was calculated to be 2.3 gram/cm³. Density of silica at this temperature is around 2.2 gram/cm³, which is quite similar.
- Raw perlite was ball milled and sifted to make it a clear fine powder. Expansion studies were conducted where several samples were placed inside a laboratory furnace at 870°C for different durations. SEM images of particles showed that particles did not expand but they only started to swell. It was seen that there was

no significant change in particle size. A further study was designed based on the assumption that if perlite particles size was reduced to nano-scale using attrition milling method and then applied heat, expansion would be observed instead of only swelling.

- Using an Attrition Mill, perlite particle size was reduced. In this procedure, attrition milling parameters were adjusted. Dynamic Light Scattering results showed that after 90 minutes of milling, size of expanded perlite became 260 nm, while size of unexpanded perlite became 238 nm. When DLS spectra obtained after 90 and 120 minutes of milling were examined, it was seen that although there is no significant change in average particle size, there is a wider spread of size after 120 minutes of milling time, which suggests that after 120 minutes there are way more bigger and smaller particles in number in the suspension than the one obtained after 90 minutes of milling. Another possible conclusion was such that agglomeration played a vital role in particles milled beyond 90 minutes as they were getting smaller until 120 minutes of run time. Although smaller particles existed in suspension obtained after 120 minutes, optimum run time was found out as 90 minutes. Also, SEM characterization of milled perlite particles showed that average particle size was actually smaller than 100 nanometers (around 40-50 nm).
- Expansion character of nano raw perlite was studied using a Hot Stage Microscope. However, there was no expansion in perlite structure. Because the heating speed of the Hot Stage Microscope was slow, process was not able to expand perlite. It was found out that only rapid heating can cause perlite to expand 5-20 times its original volume.
- Nano raw perlite samples were expanded in a laboratory furnace at various temperatures and using SEM an analysis was made. It was seen that there was no significant change in the size of observed particles, but in fact perlite particles were becoming more oval, which were due to a sintering effect. Densities of perlite samples which were expanded were analyzed using a pycnometer. As a general trend, there was reduction in perlite densities, and the decrease in density was thought to be an indication of porous structure formation inside perlite particles, when raw perlite is expanded right after being attrition milled.

- Using Hexamethyldisilazane, perlite surface was treated to make it more compatible with PDMS. Surface modified nano-perlite was then characterized using FT-IR and TGA. It was seen FT-IR results that Si-OH vibrational stretch peak intensity decreased with the increasing curing temperature. This meant that hydroxyl groups that exist on perlite surface created O-Si-O functional groups, which were desired as an aftermath of this process. It was seen in TGA analyses that as a result of Hexamethyldisilazane application on perlite surface and heat treatment, weight loss was increasing in samples as the curing temperatures of corresponding samples increased; it was seen that there was a direct relationship between two factors. The fact that weight loss increased in samples meant that organic parts on perlite surface were formed because of the surface modification.
- In rheology studies, it was seen that the third masterbatch was quite close to the target masterbatch in its elastic (G') and viscous (G'') moduli. It was seen that the number of interactions between perlite particles was increasing, and that nano expanded perlite provided more surface area to create more interactions between the polymer and the filler due to having small radius. In addition, the fourth elastomer (in section 4.6.4.) had as much network as the target masterbatch due to higher filler loading level, which accounted for more silicone-perlite interactions in the system.
- Mechanical results were very promising especially when tensile, tear strength values and elongation at break percentages were pretty close to each other. It could be seen however that with the increasing level of filler loading, elongation at break continued to go down, and there appeared to be a 20 % difference between the target elastomer formulation and the fourth formulation (in section 4.6.4.).
- There were a few reasons why mechanical properties of the nano perlite filled elastomers were close to the mechanical properties of target elastomer. First of all, expanded perlite was first nano-scaled to attain smaller particles and its surface was improved by a treatment process; this created many enhanced interactions and compatibility between the filler and the polymer. Perlite's flake/platelet shape accounted for an higher aspect ratio compared to silica. Because of this platelet structure, stress transferred from the polymer matrix was able to be transmitted to a larger surface area when compared to silica and hence

stress applied to the polymer was able to be distributed more homogeneously. Furthermore, due to the surface modification using Hexamethyldisilazane, perlite was wetted by the polymer matrix much easier, agglomeration was avoided and perlite mixed more homogeneously with the matrix.

- In SEM images of the cured elastomers, it was seen that nano-scaled perlite formed rare agglomerations which were 30-40 microns in diameter. This type of agglomeration might naturally have had negative effects on the mechanical properties of the elastomer, which were observed in mechanical results. However, it was seen that particle distribution was good overall and particles were homogeneously distributed.

5.2. Road Map

As further steps in this study, it is possible to design new experiments where perlite expansion is thoroughly studied so that nano particles are able to expand when they are subjected to rapid heating. Also, how much surface modification helps in raising the mechanical properties of PDMS-Silica composites could be further investigated. Process regarding masterbatch preparation could also be looked at and improved to avoid time delays, problems in mixing and overcome safety threats.

References

- [1] M. Dogan, M. Alkan, Some physicochemical properties of perlite as a adsorbent, *Fresenius Environ. Bull.* 13 (3b) (2004) 251–257.
- [2] P.W. Harben, R.L. Bates, *Industrial Minerals Geology and World Deposits*, Metal Bulletin Inc., London, 1990, p. 184.
- [3] S.S. Uluatam, *J. AWWA* 70 (1991) 70.
- [4] O. Demirbas, M. Alkan, M. Dogan, The removal of victoria blue from aqueous by adsorption on a low-cost material, *Adsorption* 8 (2002) 341–349.
- [5] C.W. Chesterman, *Industrial Minerals and Rocks*, fourth ed., AIME, New York, 1975, p. 927.
- [6] P. Leroy, A. Revil, A triple-layer model of the surface electrochemical properties of clay minerals, *J. Colloid Interface Sci.* 270 (2004) 371–380.
- [7] P. Somasundaran, D.W. Fuerstenau, Mechanisms of alkyl sulfonate adsorption at the alumina–water interface, *J. Phys. Chem.* 70 (1966) 90. Fig. 9. A schematic illustration of the structure of EDL of perlite. M. Alkan et al. / *Microporous and Mesoporous Materials* 84 (2005) 192–200 199
- [8] K.S. Ma, A.C. Pierre, Clay sediment-structure formation in aqueous kaolinite suspensions, *Clays Clay Miner.* 47 (1999) 522.
- [9] D. Penner, G. Lagaly, Influence of organic and inorganic salts on the coagulation of montmorillonite dispersions, *Clays Clay Miner* 48 (2000) 246.
- [10] J.R. Hunter, *Introduction to Modern Colloid Science*, Oxford Science Publications Oxford University Press Inc., New York, 1993.
- [11] I. Sondi, J. Biscan, V. Pravdic, Electrokinetics of pure clay minerals revisited, *J. Colloid Interface Sci.* 178 (1996) 514–522.

- [12] I. Sondi, O. Milat, V. Pravdic, Electrokinetics potentials of clay surfaces modified by polymers, *J. Colloid Interface Sci.* 189 (1997) 66–73.
- [13] A. Delgado, F. Gonzalez-Caballero, J.M. Bruque, On the zeta potential and surface charge density of montmorillonite in aqueous electrolyte solution, *J. Colloid Interface Sci.* 113 (1) (1986) 203–211.
- [14] D.J.A. Williams, K.P. Williams, Electrophoresis and zeta potential of kaolinite, *J. Colloid Interface Sci.* 65 (1) (1978) 79–87.
- [15] A. Fernandez-Nieves, F.J. de las Nieves, The role of ζ potential in the colloidal stability of different TiO₂/electrolyte solution interfaces, *Colloid Surf. A: Physicochem. Eng. Aspect* 148 (1999) 231–243.
- [16] B. Ersoy, M.S. Celik, Electrokinetic properties of clinoptilolite with mono- and multivalent electrolytes, *Micropor. Mesopor. Mater.* 55 (2002) 305–312.
- [17] G. Xu, J. Zhang, G. Song, Effect of complexation on the zeta potential of silica powder, *Powder Technol.* 134 (3) (2003) 218–222.
- [18] C.J. Yu, Z.T. Jiang, H.Y. Liu, J. Yu, Influence of solvation interactions on the zeta potential of titania powders, *J. Colloid Interface Sci.* 262 (2003) 97–100.
- [19] M.S. Celik, E. Yasar, Electrokinetic properties of some hydrated boron minerals, *J. Colloid Interface Sci.* 173 (1995) 181–185.
- [20] R. Nyström, M. Linden, J.B. Rosenholm, The influence of Na⁺, Ca²⁺, Ba²⁺, and La³⁺ on the ζ potential and yield stress of calcite dispersions, *J. Colloid Interface Sci.* 242 (2001) 259–263.
- [21] G. Yin, Z. Liu, J. Zhan, F. Ding, N. Yuan, Impacts of Surface charge property on protein adsorption on hydroxyapatite, *Chem. Eng. J.* 87 (2002) 181–186.

- [22] Alexandre, M.; Dubois, P.; Sun, T.; Garces, J. M.; Jerome, R. *Polymer* 2002, 43, 2132.
- [23] Zilg, C.; Meulhaupt, R.; Finter, J. *Macromol. Chem. Phys.* 1999, 200, 661.
- [24] Reichert, P.; Nitz, H.; Klinke, S.; Brandsch, R.; Thomann, R.; Meulhaupt, R. *Macromol. Mater. Eng.* 2000, 275, 8.
- [25] Lu, H.; Liang, G.-Z.; Ma, X.; Zhang, B.; Chen, X. *Polym. Int.* 2004, 53, 1545.
- [26] Wang, Z.; Pinnavaia, T. *Chem. Mater.* 1998, 10, 3769.
- [27] Shah, D.; Maiti, P.; Gunn, E.; Schmidt, D. F.; Jiang, D. D.; Batt, C. A.; Giannelis, E. P. *Adv. Mater.* 2004, 16, 1173.
- [28] Liu, W.; Hoa, S. V.; Pugh, M. *Polym. Eng. Sci.* 2004, 44, 1178.
- [29] Shah, D.; Maiti, P.; Gunn, E.; Schmidt, D. F.; Jiang, D. D.; Batt, C. A.; Giannelis, E. P. *Adv. Mater.* 2004, 41, 3264.
- [30] Grulke, E. A. In *Polymer Handbook*, 4th edition; Brandrup, J., Immergut, E. H., Grulke, E. A., Abe, A., Bloch, D. R., Eds.; John Wiley & Sons: New York, 2005; Chapter VII.
- [31] Cohen Addad, J.-P. *Surf. Sci. Ser.* 2000, 90, 621.
- [32] Burnside, S. D.; Giannelis, E. P. *Chem. Mater.* 1995, 7, 1597.
- [33] Wang, S.; Li, Q.; Qi, Z. *Key Eng. Mater.* 1998, 137, 87.
- [34] Wang, S.; Long, C.; Wang, X.; Li, Q.; Qi, Z. *J. Appl. Polym. Sci.* 1998, 69, 1557.
- [35] Takeuchi, H.; Cohen, C. *Macromolecules* 1999, 32, 6792.

- [36] Anastasiadis, S. H.; Karatasos, K.; Vlachos, G.; Manias, E.; Giannelis, E. P. *Phys. Rev. Lett.* 2000, 84, 915.
- [37] Burnside, S. D.; Giannelis, E. P. *J. Polym. Sci. B: Polym. Phys.* 2000, 38, 1595.
- [38] LeBaron, P. C.; Pinnavaia, T. J. *Chem. Mater.* 2001, 13, 3760.
- [39] Wang, J.; Chen, Y.; Jin, Q. *Macromol. Chem. Phys.* 2005, 206, 2512.
- [40] Kaneko, M. L. Q. A.; Yoshida, I. V. P. *J. Appl. Polym. Sci.* 2008, 108, 2587.
- [41] Simon, M. W.; Stafford, K. T.; Ou, D. L. J. *Inorg. Organomet. Polym.* 2008, 18, 364.
- [42] Daniel F. Schmidt and Emmanuel P. Giannelis: "Silicate Dispersion and Mechanical Reinforcement in Polysiloxane/Layered Silicate Nanocomposites", *Chem. Mater.* **22** (2010), 167-174.
- [43] Lina Dai, Zhijie Zhang, Yunfeng Zhao, Hongming Liu and Zemin Xie: "Effects of Polymeric Curing Agent Modified with Silazanes on the Mechanical Properties of Silicone Rubber", *Journal of Applied Polymer Science*, Vol. **111** (2009), 1057-1062.
- [44] Manuela L. Q. A. Kaneko, Inez V. P. Yoshida: "Effect of Natural and Organically Modified Montmorillonite Clays on the Properties of Polydimethylsiloxane Rubber", *Journal of Applied Polymer Science*, Vol. **108** (2008), 2587-2596.
- [45] Liliane Bokobza: "Elastomeric Composites. I. Silicone Composites", *Journal of Applied Polymer Science*, Vol. **93** (2004), 2095-2104